AN ABSTRACT OF THE THESIS OF

Paul Allister Covert for the degree of Master of Science in Oceanography presented on May 7, 2001. Title: An Examination of the Form and Variability of Manganese Oxide in Columbia River Suspended Material.

Abstract approved: Signature redacted for privacy.

Fredrick G. Prahl

Suspended particulate matter (SPM) in the Columbia River is a mixture of particles of several origins having varying physical and biogeochemical properties. The relative abundances of these freshwater particles changes with season and apparently also with tide. Prior investigation has quantified seasonal variation of organic material in both the Columbia and Willamette rivers. In this investigation, seasonal variability in the abundace of manganese in the mineral fraction (Mn/Al) is confirmed in both rivers. Mn/Al hovers around 0.01 (crustal average = 0.011, Whetten et al., 1969) during the winter and early spring, rising in the spring and summer to 0.04 and 0.06 in the Columbia and Willamette Rivers, respectively. Results from particle settling experiments and electron microprobe photos of SPM indicate that seasonal Mn/Al variability is a result of addition of Mn-oxides to SPM in the summer months, and that these oxides exist as discrete, slow settling particles.

A short-term (12 hour) variability of Mn/Al, as well as Chl *a*/POC, is observed at mid-depth in the Columbia River. Owen Tube particle settling experiments revealed that with respect to geochemical properties, SPM could be divided into two settling classes: slow (<0.11 cm/s) and fast (>0.11 cm/s). Particles in the slow settling class were typically

enriched in Mn and Chl *a* , while fast settling particles were more characteristic of detrital material. One consequence of this geochemical separation is that it leads to differential particle settling and resuspension in the tidal freshwater portions of the river, resulting in the observed 12-hour variability of SPM character. Such variability could have further reaching consequences with regard to chemical transport and dispersal.

An Examination of the Form and Variability of Manganese Oxide in Columbia River Suspended Material

by

Paul Allister Covert

A THESIS
submitted to

Oregon State University

in partial fulfillment of
the requirements for the
degree of

Master of Science

Completed May 7, 2001
Commencement June 2002

ACKNOWLEDGMENTS

As I prepare to finish the revisions to this thesis, only to embark on a Ph.D. program tomorrow, thanks are due to all those who have helped and guided me along the way. First and foremost, I want to acknowledge and thank Fred Prahl for being an excellent mentor and good friend over the past four years. I arrived at COAS as a lab chemist, and making the transition to a field science, where the environment is not nearly as controlled as it is in a beaker, was frustrating a lot of the time. Without Fred's advice, support, and discussions over coffee and beer, I could not have made this transition.

I also want to thank Margaret Sparrow, Bobbi Conard, and Andy Ungerer for helping me with the analytical aspects of this thesis. In addition, Margaret's humor and sarcasm always makes life in the lab more bearable.

Finally, I want to thank Melissa for deciding to come to COAS, instead of UW. She was there whenever I needed moral support. She provided the encouragement I needed to finish when my interest was waning. And, she was a great partner in crime whom I could go do anything unrelated to school with.

TABLE OF CONTENTS

TABLE OF CONTENTS, CONTINUED

LIST OF FIGURES

LIST OF FIGURES, CONTINUED

LIST OF FIGURES, CONTINUED

LIST OF TABLES

LIST OF APPENDIX TABLES

AN EXAMINATION OF THE FORM AND VARIABILITY OF MANGANESE OXIDE IN COLUMBIA RIVER SUSPENDED MATERIAL

1: INTRODUCTION

The Columbia River and its major tributaries (i.e. Snake and Willamette rivers) have long served as an important resource for local inhabitants. They have acted as a source of food and provided a means of transportation. Within the last century, their water has been diverted for agricultural needs, and the rivers' power converted to electricity for north-western cities. Close interaction with the river provided a respect of the river and perhaps an understanding of how human actions affected the river. The importance of the Snake, Willamette and Columbia rivers are no less today. Industry lines both sides of these rivers in parts, their water is still used for irrigation, and the power generated by hydroelectric dams provides millions with electricity on a daily basis. Yet, with the complexity of life now, few can say they feel an attachment to the river, and even fewer can say that they understand how humans are affecting the river. Given the huge impact of the Columbia river (perceived or not) on our lives, it is only fair (not to mention, important) to understand the huge impact of our lives on the river.

What does this have to do with manganese? This work does not directly investigate the effects of human activities on the river. The goals of this thesis were to investigate seasonal behavior and forms of particulate manganese in the Columbia and Willamette rivers. In its oxidized form, manganese is intimately linked to human influences in that it could act as an efficient contaminant "sponge," adsorbing dissolved trace metal species present in the river (e.g. Stumm and Morgan, 1970; Hem, 1978). With respect to trace

metals in the Columbia and Willamette Rivers, the U.S. Geological Survey (USGS) has reported high levels of mercury, chromium, and arsenic in the Willamette river (Fuhrer et al., 1994). By improving our understanding of the forms and variability of particulate manganese in these river systems, we can better understand how future actions could impact the river and surrounding wetlands and ecosystems.

The presentation and discussion of the results has been divided into two process-oriented chapters, seasonal variability and diurnal variability. This division was done because conceptually this is an easy way to break down the complex issue of SPM composition and variability. This, however, is not meant to imply that the two processes described by these chapters are independent of each other. Several times it is necessary to refer to results from the other chapter in order to add weight to an argument. This results in the awkward situation of occasionally referring to results from a later chapter in the thesis. The concluding chapter reintegrates the two processes into one description of river-borne SPM and implications of variability on contaminant transport to the Columbia River estuary.

2: METHODS AND MATERIALS

2.1 Sample collection and treatment

The goal of sample collection was to provide data with sufficient resolution so that interpretation on both seasonal and daily time scales was possible. In order to do this without collecting an unmanageable number of samples, two different schemes were employed: (1) sample collection on a bi-monthly to monthly basis in cooperation with the U.S. Geological Survey's (USGS) NAtional Stream Quality Accounting Network (NASQAN) project, and (2) sample collection every two hours during two to three week long, seasonal cruises, as part of the Columbia River Land-Margin Ecosystem Research (LMER) Program.

NASQAN -- Samples collected in cooperation with the NASQAN project were taken from the Columbia River at the Beaver Army Terminal (85 km or 53 miles upriver of the mouth), henceforth referred to as RM53, (46°10'54" N, 123°10'58" W) and the Willamette River immediately downstream of the Morrison Bridge in Portland, OR, identified as WRM12.8, (45°31'04" N, 122°40'07" W) (Fig. 2.1). These locations were chosen for several reasons. Beaver Army Terminal is the first location upriver of the estuary that is uninterrupted by islands where the channel is narrow and is above the furthest point of tidally driven salt intrusion into the river. The Morrison Bridge sampling location was chosen to be far enough from the confluence of the Willamette and Columbia rivers so as to avoid any tidally driven backflow of the Columbia into the Willamette (Rickert, 1984).

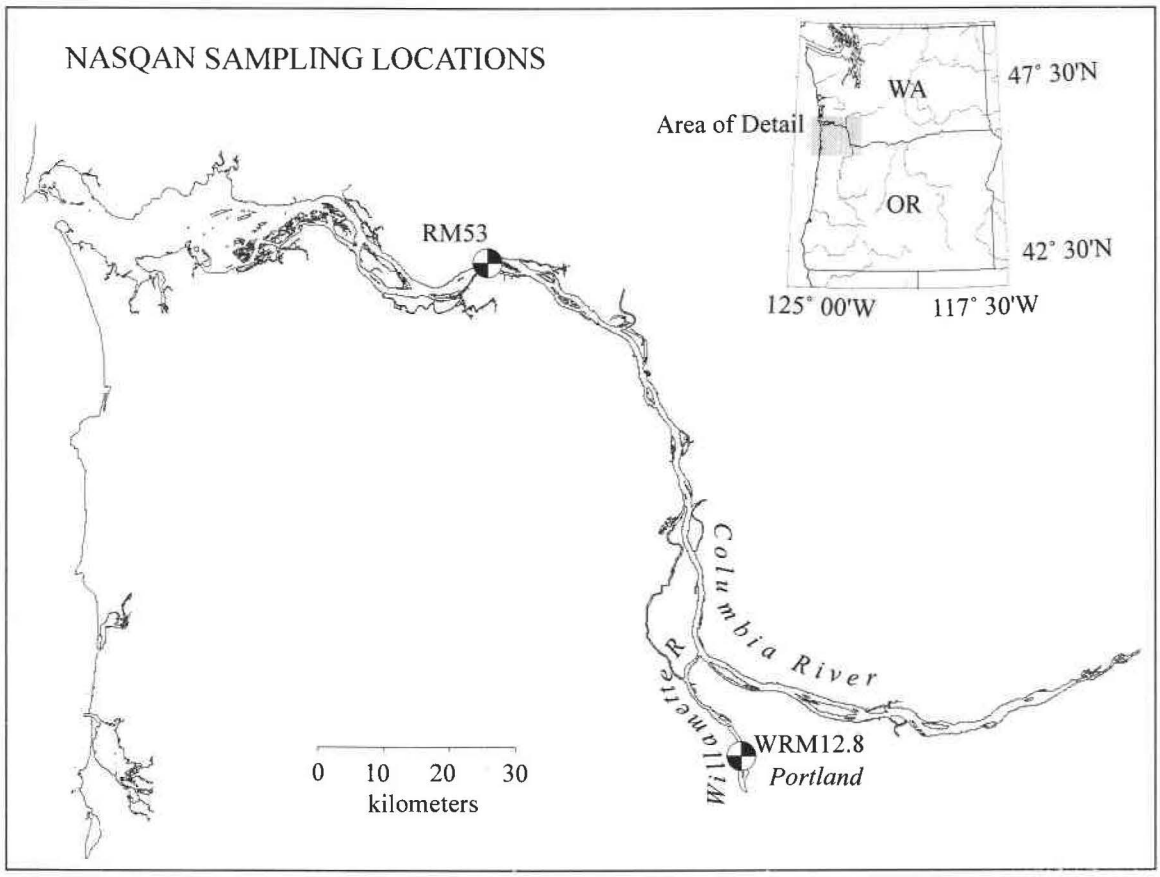

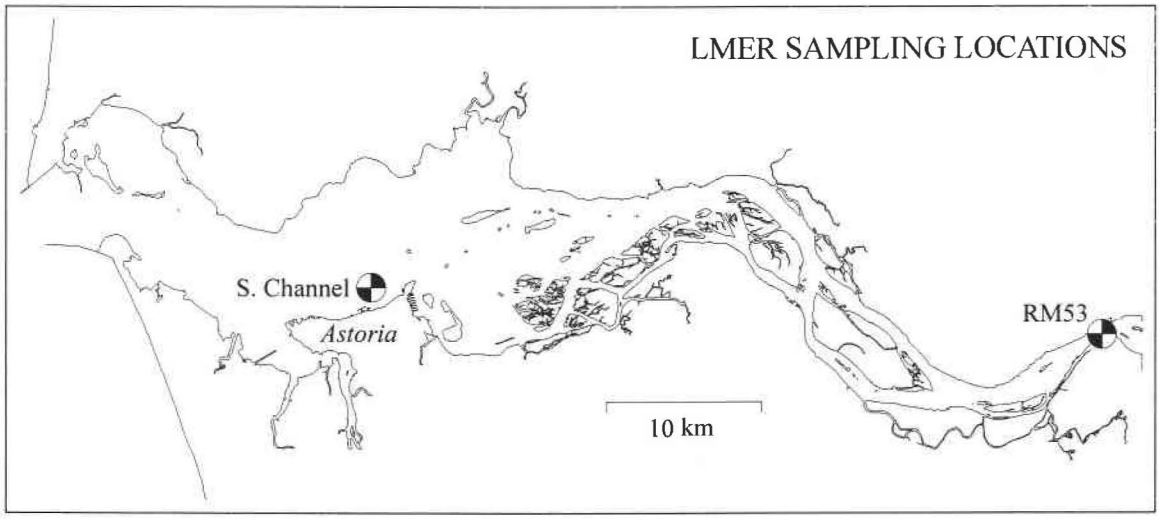

Fig. 2.1: Sampling locations from the NASQAN and LMER programs in the Columbia River, Willamette River, and Columbia River estuary.

Sample collection with the NASQAN program was done aboard a USGS boat equipped with a hydraulic winch. At each of five evenly spaced locations spanning the river channel, an 8 L, collapsible Teflon collection bag attached to a Teflon nozzle was lowered to the river bottom and raised at a constant velocity, yielding a flow and depth weighted (isokinetic) sample. In addition to sample collection, channel depth, surface velocity, temperature, pH, conductivity, and dissolved oxygen, were measured at each location. Each of the samples collected from the five locations were combined in an acid-washed polyethylene carboy. This somewhat time-consuming sampling procedure (isokinetic sampling) was designed so that the resulting sample is a cross-sectional and flow-weighted representation of the river (Edwards and Glysson, 1988; Fuhrer et al., 1996). Water samples were kept dark and transported to OSU or USGS laboratories, filtered within 6 hours of sample collection, and stored for analysis .

Isokinetic sample collection is vital for flux estimates. Although flux estimates are not part of this thesis, isokinetic sampling likely yields a better geochemical description of SPM as well, due to flow and depth differences across the river channels. The Columbia River is nearly uniform in depth across the channel at RM53, but due to the curvature of the river at this location, velocities near the north shore are generally 1.5 to 2 times the velocities near the south shore. On the Willamette River, velocities are nearly uniform across the channel, but the eastern edge of the channel is approximately 5 meters shallower than the western edge.

LMER – Sample collection during the LMER cruises was performed at RM53 and Buoy 39 (46°12'03"N, 123°49'05' W) (Fig. 2.1) in the South Channel of the Columbia

River Estuary. Water and suspended particulate material (SPM) samples were collected aboard the *RV Robert Gordon Sproul* and *RV Wecoma* at mid-depth at RM53, and at surface and bottom depths in the north and south channels in the estuary, and near the mouth of the estuary (Fig. 2.1). Samples were collected by employing a high volume submersible pump attached to a conductivity-temperature-depth (CTD) profiler equipped with optical backscatter (OBS) and AC-9 fluorescence sensors (Simenstad et al., 1994).

2.2 Ultrafiltration

Several times during the LMER cruises, large amounts of SPM were collected (> 1 g). This was accomplished by extracting SPM from 60-80 L of water. Large volumes of water were collected by the method described in section 2.1. This water was passed through a 64 μm mesh to remove material that would clog the ultrafiltration unit. The >64 μm fraction captured by the sieve was washed into a sample jar and frozen. The remaining sediment, <64 μm fraction, was concentrated into approximately 1 L of water with a Millipore® tangential flow filtration system (Hernandez & Stallard, 1998), equipped with a 0.45 μm pore size Pellicon® cartridge, running in a recirculation mode. The remaining water was removed by centrifugation. The sediment was then placed into a sample jar and frozen. Back on shore, samples were freeze-dried, homogenized using a ball mill, and stored for analysis.

2.3 Particle settling experiments

A bottom withdrawal tube (Fig. 2.2) was used to investigate the effects of particle settling on SPM composition. Using this device, it is possible to collect a relatively undis-

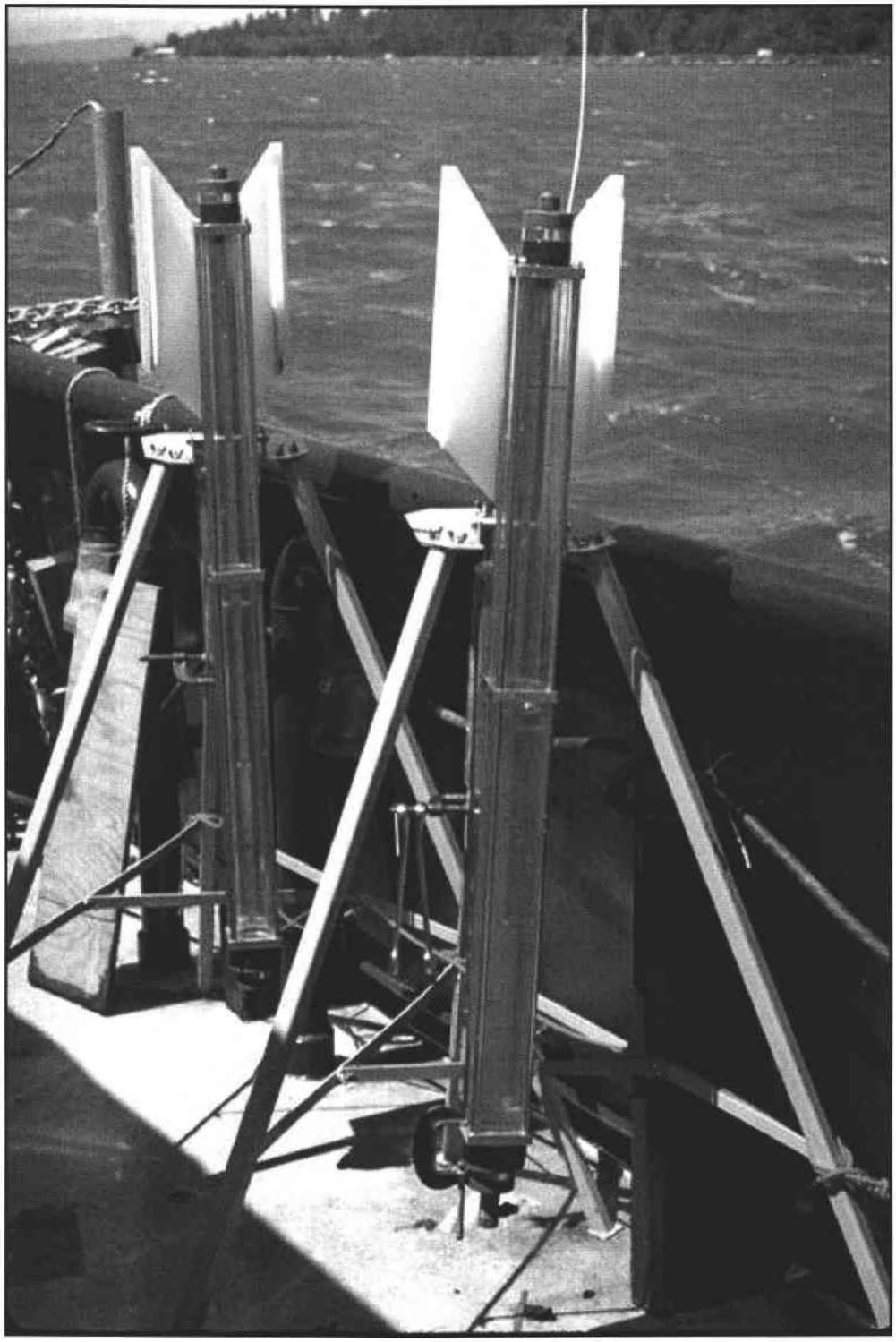

Fig. 2.2: Braystoke SK-110 water sampler in vertical position on deck. Samples were withdrawn from the bottom of the tube through a spigot on the end cap.

turbed sample from the water column and determine settling velocities and size distribution of particles and flocs comprising the SPM. The bottom withdrawal tube used is a 1 meter long, 5 cm diameter Braystoke SK-110 water sampler (Simenstad et al., 1994; Reed and Donovan, 1994), which is a modification of the Owen Tube (Owen, 1976). The interior of the bottom end cap was further modified such that it was conical in shape. This allowed the settling sediment to focus on the spigot, minimized currents that could lead to resuspension of settled particles, and prevented buildup of sediment around the bottom cap. The total volume of the tube is 2 L.

For sampling, the tube is lowered into the water to mid-depth. Stabilizing fins on the tube align the axis of the tube with the flow of the river in a horizontal position, allowing the water to flow through the tube. A messenger sent down the wire caps the ends of the tube, and the tube is raised in a horizontal position to the deck. Once on deck, the tube is turned vertical, placed on a support frame, and sample collection is begun.

At eight prescribed times, measured from the time the tube was turned vertical, samples of approximately 250 mL were taken from the bottom of the tube. Sampling times were chosen on the basis of approximate Stokes' settling times required to capture spherical sand particles of varying size (Reed and Donovan, 1994). Each of the aliquots were vacuum filtered onto pre-weighed polycarbonate filters (Gelman Sciences 47 mm diameter, 0.45 μm pore size). Filters were oven dried (24 hours at 40-50°C), weighed to determine SPM concentration (mg sediment/mL water), and analyzed for metal content via the procedure outlined in section 2.6.

2.4 Odén Curve calculations

Analysis of the chemical composition of Owen Tube fractions yields a qualitative feel for the size and chemical distribution of particles composing SPM. However, in order to obtain a quantitative description of the particle field, some manipulation of the data is needed. Each fraction collected from the Owen Tube contains a mixture of particles of varying size, density, and consequently, settling velocity. To obtain a description of the amount and character of particles in a given settling velocity range, some means is needed to deconvolute the raw data from the Owen Tubes. Since this is a complex procedure, the best way to describe the theory is through an example.

Imagine the system of particles shown in Fig. 2.3. Particles of three different settling velocities (4v, 2v, and v) comprise the system. At time zero, the particles are uniformly dispersed throughout the tube. Given that the particles, ranging from largest to smallest, settle 40, 20, and 10 cm in time T, respectively, then the resulting distribution of particles in the Owen Tube will be as shown in figure 2.3a-d. It is clear from the figure that if one were to collect sediment from the bottom of the tube at time T, the sample collected would contain all three types of particles. At time 5T, however, only the two slower settling particles will be in the sample, as the largest of the particles had completely settled out of the tube by time 2.5T. The end result is that you have several samples, each with a different mass, but none representing the starting mass of one type of particle.

The mass of the accumulated particles is constantly changing with time. A graphical representation of this process can be prepared (Fig. 2.4). This presentation of the data is called the Odén curve (Odén, 1924). The segment of the curve from T_0 to 2.5 T represents the time during which all sizes of particles are settling to the bottom of the tube. The slope

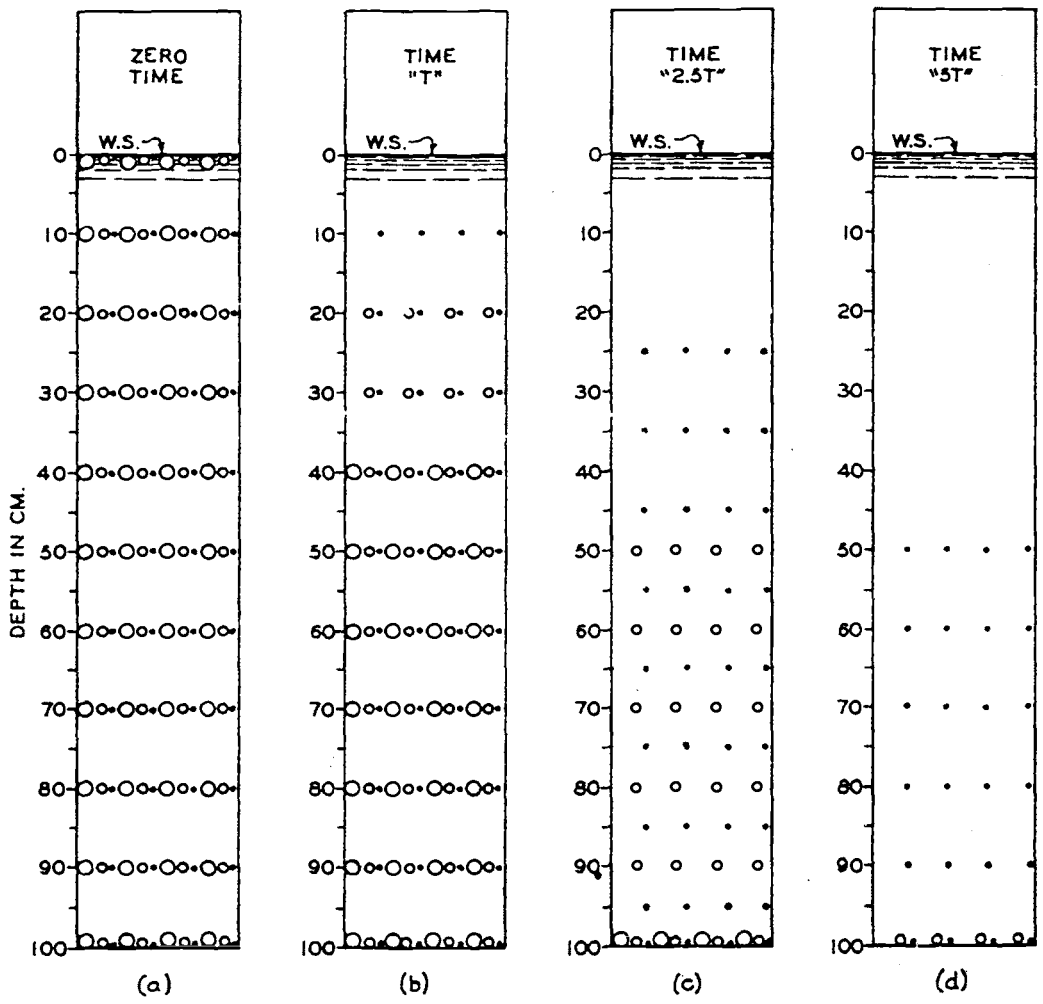

Fig. 2.3: A system of particles in suspension. Adapted from Army Corps of Engineers (1946) publication. Three different particle diameters are shown, designated from largest to smallest as d_1, d_2, and d_3. Their respective settling velocities are 4v, 2v, and v.

of the line represents the accumulation rate. After all of the largest particles have settled out, the accumulation rate decreases to a rate that remains constant until all of the mid-sized particles settle out.

The hypothetical example illustrated in Figs. 2.3 and 2.4 describes a particle field composed of particles with three distinct settling velocities. In reality, the particle field contains particles whose settling velocities span a continuum ranging from permanently

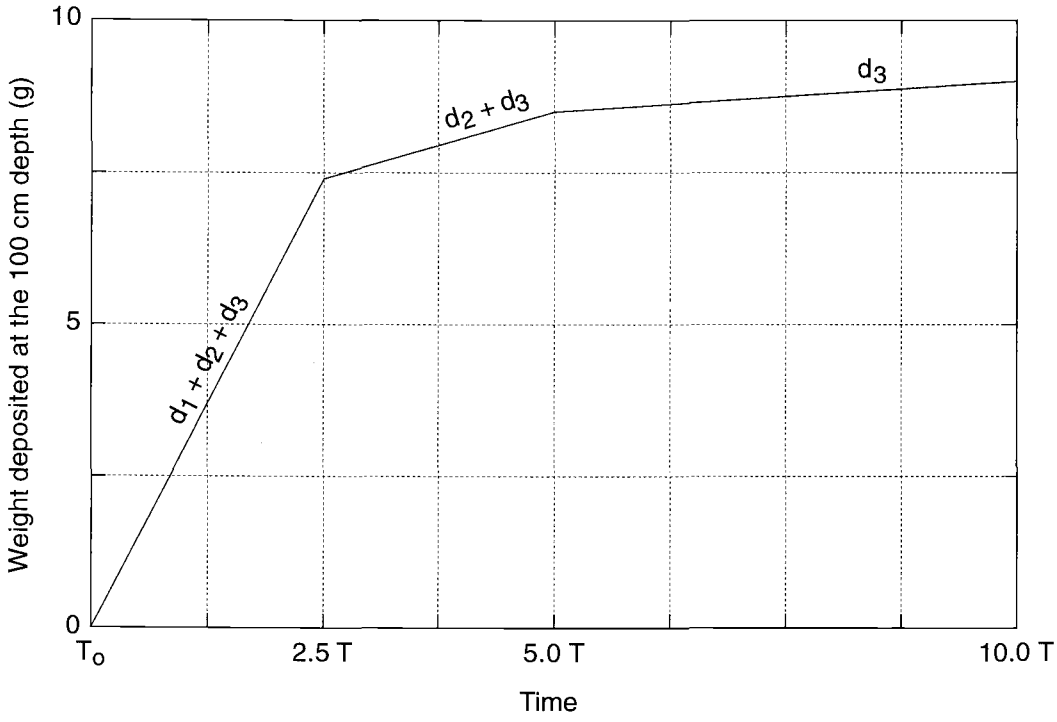

Fig. 2.4: Mass accumulation curve of the settling experiment shown in Fig. 2.3. Adapted from Army Corps of Engineers (1946).

suspended to rapidly settling. This continuum yields a smooth Odén curve that can be described by the integral form of the Rosin-Rammler-Sperling-Bennet (RRSB) distribution:

$$\mu_t = 1 - \exp\left(-\left(\frac{t}{n}\right)^{\sigma}\right) \qquad \text{(eq. 2-1)}$$

where μ_t is the cumulative mass of material settled at time t, n is the position parameter, and s is the scattering parameter (Niedergesäss et al., 1996). It can be shown that the value of the y-intercept of the tangent to the Odén curve at any time, t, is equal to the weight of the sediment in the entire sample with settling velocity greater than v, where v is defined as the height of the tube divided by t (see Odén, 1924 and Army Corps of Engineers, 1946). This relation that makes it possible to bin the mass or chemical composition of the SPM into settling velocity ranges. In practice, this was accomplished by first fitting the

cumulative mass accumulation, μ_t (e.g. mass of fraction 1, mass of fractions 1+2, etc.) versus t data to equation 2-1. Y-intercepts of the tangents to the fitted Odén curve were then obtained at t equal to 345, 1158, and 2436 s (settling velocities of 0.22, 0.044, and 0.011 cm/s, respectively). The fraction of sediment settling within a given velocity range was then obtained by calculating the differences between the y-intercepts. For example, to obtain the fraction of sediment with settling velocity between 0.044 and 0.011 cm/s, subtract the y-intercept of the tangent at t = 1158 s from that at t = 2436 s. This procedure was followed to obtain settling velocity distributions for both bulk masses and elemental masses.

2.5 SPM concentration

The concentration of the bulk suspended material (mg sediment/L water) was determined by pressure filtering (N_2, $\approx$ 100 kPa) a measured volume (2-3 L) of water through a pre-weighed polycarbonate membrane filter (Poretics 90 mm diameter, 1.0 μm pore size). The loaded filters were folded into eighths, placed into clean petri dishes and oven dried for at least 24 hours at 40-50°C. Dried filters were re-weighed, and SPM concentration calculated as the weight difference between the loaded and unloaded filters, divided by the volume of water filtered. Analytical precision is shown in Table 2.1.

2.6 POC/PN measurement

SPM was loaded onto precombusted (450 °C, $\approx$ 4 h.) glass fiber filters (25 mm dia. GF/F, Whatman) by vacuum filtering a known volume (200-500 mL) of water. These filters were oven dried (60 °C for 24 h) and stored in clean plastic petri dishes until analysis.

Table 2.1: Precision and accuracy of SPM and trace metal analyses.

	SPM conc. (mg/L)	Al (wt%)	Fe (wt%)	Mn (ppm)
	Beaver Army Terminal 11/30/99 (N = 5)			
$\bar{x}$	48	9.4	5.89	1090
1σ	4	0.7	0.21	40
RSD	8%	7%	3.6%	4%
		BCR-3 (N = 11)		
$\bar{x}$		7.4	9.5	1494
1σ		0.5	0.5	108
RSD		7%	5%	7%
		BCR-3 (reported values)		
		7.22	9.29	1,394

Analysis for particulate organic carbon (POC) and nitrogen (PN) was performed in the laboratory by high temperature combustion using a Carlo Erba NA-1500 CNS analyzer. Actual measurements are of total particulate carbon and nitrogen, as fuming of the samples with concentrated HCl to remove inorganic carbon was not performed. However, a comparison of carbon numbers obtained from both fumed and non-fumed samples in prior studies of Columbia River SPM indicate a negligible amount of inorganic carbon (Prahl et al., 1998). Reproducibility of replicate samples was typically ± 5% or better.

2.7 Metals analysis

Sediments were analyzed for total Mn, Fe, and Al. Several were also analyzed for total Cu and Zn. Sediments that were collected on nucleopore filters were placed in quartz crucibles (Fisher, 30 mL) and heated at 550°C to completely combust the filter, leaving only the mineral ash in the crucible.

All digestions were performed in acid cleaned (10% hot HNO_3, overnight) teflon vials (Savillex, 15 mL). Sediment (< 25 mg) was placed into the vials, and 1 mL each of high purity, concentrated HNO_3 (quartz distilled) and HF (Aldrich, 48 wt.% in water, double distilled) were added. The vials were sealed and placed in an oven (85-90°C) overnight. Following the overnight heating, each Savillex Vial lid was rinsed twice with 6N HCl (GFS, double distilled) and added to the HNO_3/HF digestion. The digested samples were evaporated to a bead (2-3 mm in diameter at the bottom of the vial) with a hotplate set on low heat, being careful to not let the digestion evaporate to dryness. This evaporation procedure was repeated three times, once after each of the following sequential additions: 500 μL of 6N HCl (GFS, double distilled), 500 μL of 16N HNO_3 (quartz distilled), 500 μL of 8N HNO_3 (quartz distilled). Following the final addition, 5 mL of 2N HNO_3 (quartz distilled) was added to the digestion, and the entire solution transferred to acid cleaned (overnight in 10% hot HNO_3) 8 mL Nalgene bottles for storage.

Analysis of trace metal content was performed on a Varian Liberty 150 model ICP atomic emission spectrometer (ICP-AES). All digestions were diluted 11-fold prior to analysis. The accuracy of the analytical method was determined by submitting Columbia River Basalt standard (BCR-3, in-house standard, taken from the same core as USGS BCR-1 standard) to the same digestion and analytical procedure as the SPM samples (Table 2.1). Reproducibility of the analytical procedure was determined by analyzing five replicate filters for metal contents (Table 2.1)

2.8 Electron Microprobe Analysis

Sediments collected by ultrafiltration (see section 2.2) were suspended in epoxy resin, formed into a plug and allowed to harden. The flat surface of the plug was then polished in preparation for analysis by electron microprobe (Cameca/Camebax). With the electron beam power set to 49.9 nA and 15.1 kV, characteristic K_α emissions were measured to obtain rasterized element maps (Al, Mn, Si, and Ti) of the samples (Reed, 1993).

3: SEASONAL VARIABILITY OF SPM CHARACTER

3.1 Introduction

Worldwide, the movement of particles has been recognized as an important mechanism by which contaminant organic and metal compounds are dispersed in natural systems. Of specific interest is the chemistry that occurs when suspended particulate matter (SPM) enters an estuary and encounters rapidly changing environments. A considerable amount of work has been done over the past decade to investigate the roles estuarine turbidity maxima (ETM) play in estuarine chemistry (e.g. Gobeil et al., 1981; Prahl et al., 1997). One of the keys to understanding ETM chemistry is having a good handle on the character and chemistry of particles delivered to the estuary by the river.

As part of a Land Margin Ecosystem Research (LMER) project, an investigation of riverine SPM in the Columbia River was initiated. One result of this research has been a quantification of the seasonal variability of organic material within the SPM. Organic matter varied its mass contribution to bulk SPM from 5% during the winter months up to 26% in the spring and summer. This change in mass contribution was accompanied by a shift in the origin and quality of the organic matter (for example: allochthonous to autochthonous and chlorophyll-poor to chlorophyll-rich) (Sullivan et al., 2001). However, relatively little work has been done with respect to the inorganic side of the story. The work presented in this chapter broadens the scope of the seasonality story in the Columbia and Willamette rivers by placing the patterns for inorganic and organic material side-by-side.

The little work done to date on metal content of SPM showed that over the 1995-1996 hydrologic year Mn/Al varied from approximately 0.011 to 0.030 in the Columbia

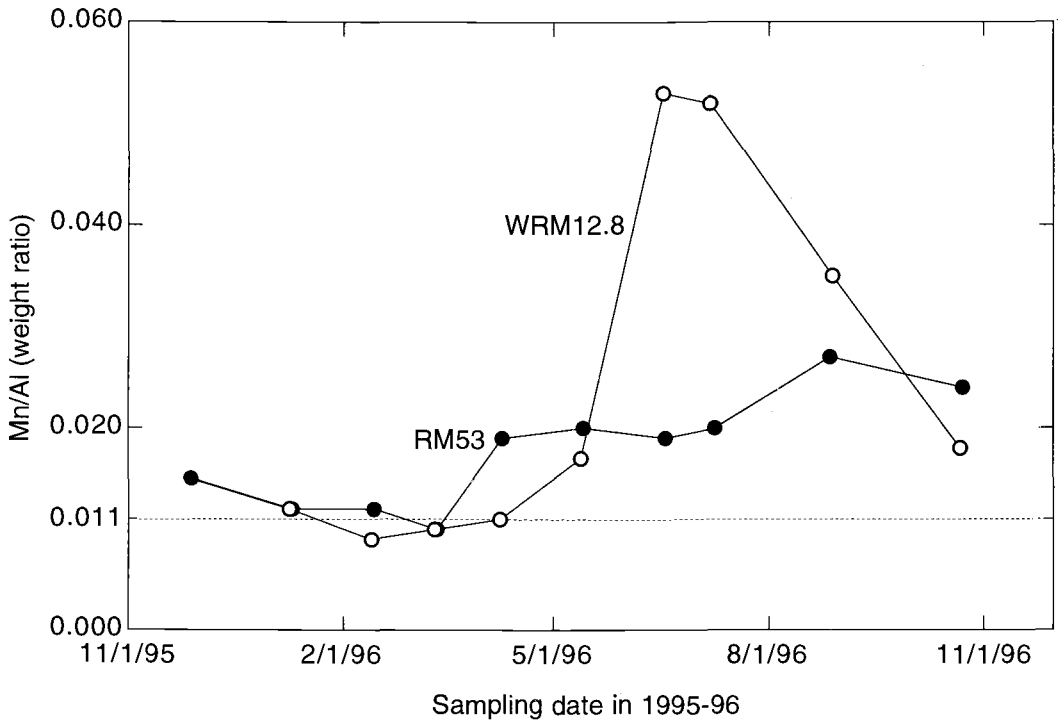

Fig. 3.1: Behavior of Mn/Al in Columbia and Willamette River SPM during 1996 (unpublished data from Sullivan, 1997 study). Horizontal dotted line at 0.011 marks Mn/Al for average crustal material (Taylor, 1964).

River and 0.011 to 0.060 in the Willamette River (Fig. 3.1) (unpublished data, Sullivan, 1997). As Sullivan's work was primarily concerned with biology and the quality of organic carbon in the two rivers, the observed Mn/Al variability remained just that, an observation. Since these data span only one year, it is not possible to assess whether or not the variability is a yearly occurrence or if it is particular to this year, a year that included river discharges far in excess of average due to a 50 year flood in February 1996 (Fig 3.2). For further investigation of seasonal variability in Mn/Al, the following two hypotheses were advanced:

(1) OCCURRENCE – Variability of Mn/Al seen in 1996 is a seasonal phenomenon, and not attributable to the 50 year flood that also occurred that year,

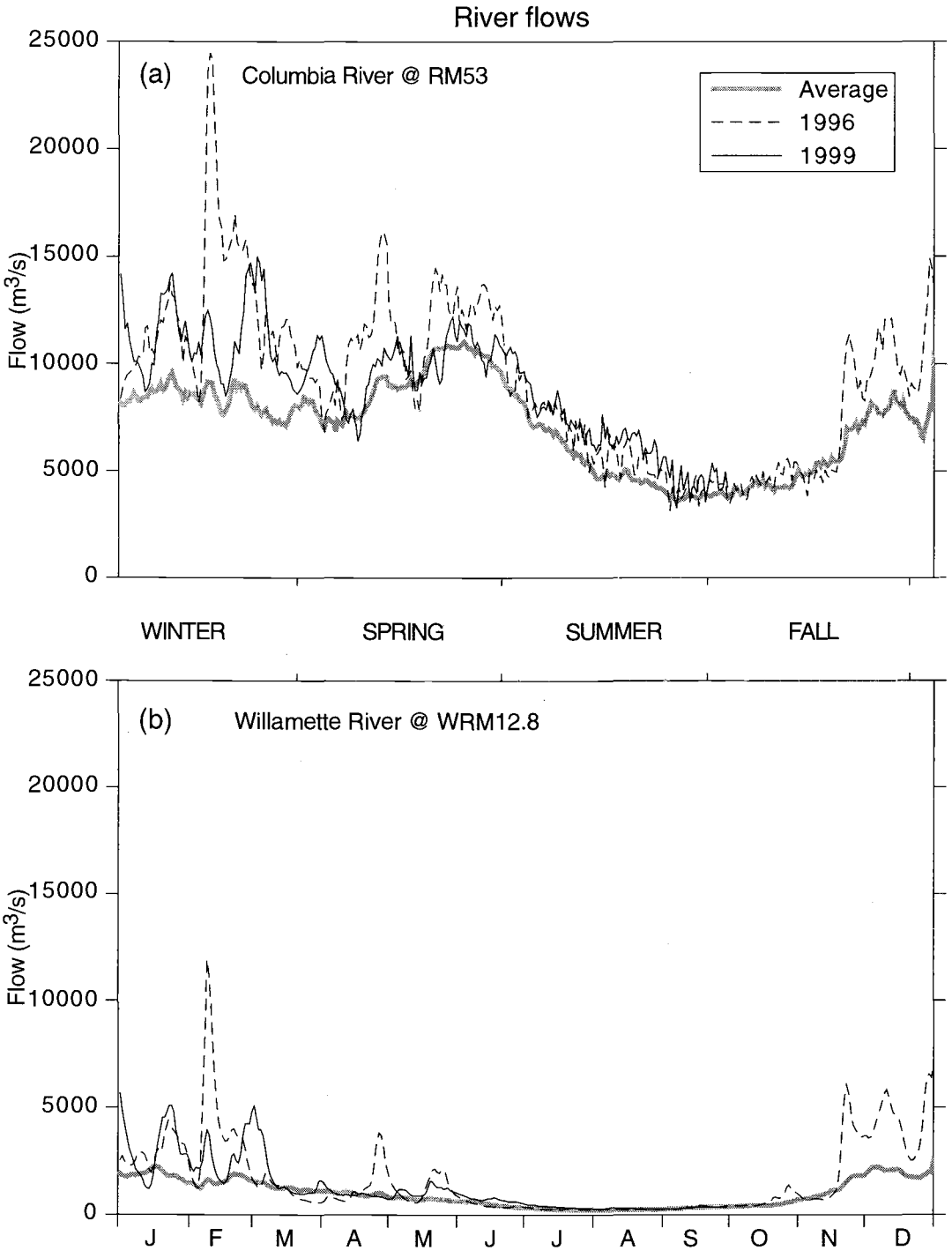

Fig. 3.2: Daily mean river flows at during 1996 and 1999 compared to the yearly average flow. (a) Columbia River at RM53. Years averaged: 1968-1970 and 1990-1999. (b) Willamette River at WRM12.8. Years averaged: 1972-1999. (USGS data, http://www.waterdata.usgs.gov)

(2) CAUSE – A seasonal difference in the amount of manganese-oxides associated with SPM is the reason Mn/Al varies on seasonal time scales.

3.2 Results

River flow, temperature, and pH – River flows on the Columbia and Willamette Rivers were closer to average in 1999 than in 1996 (Fig. 3.2). In a few instances, during winter and early spring, flows were considerably greater than the historical average, but they never approached the 25,000 m^3/s magnitude of flooding that occurred in February, 1996. In late spring through early fall, river flow deviated little from historical flows.

Temperature conditions in both the Columbia and Willamette Rivers were nearly identical during 1999 (Fig. 3.3a) (data from USGS NASQAN program). The lowest temperature measured was approximately 7°C in March, and a maximum temperature of approximately 20°C was reached in August, a pattern characteristic of these two rivers (Fuhrer et al., 1996).

The pH of both rivers, though different, nevertheless decreased in similar fashion from March to November, with two plateaus. One plateau occurred in early spring and another in the summer (Fig. 3.3b). The pH spike in the Willamette River in October remains unexplained.

POC – The percentage of particulate organic carbon in total SPM (%POC) had a seasonal response similar to the river temperature, particularly in the Willamette River (Fig. 3.4). In the Willamette, %POC uniformly increased to a maximum in August and then uniformly decreased through November. Columbia River %POC also increased in

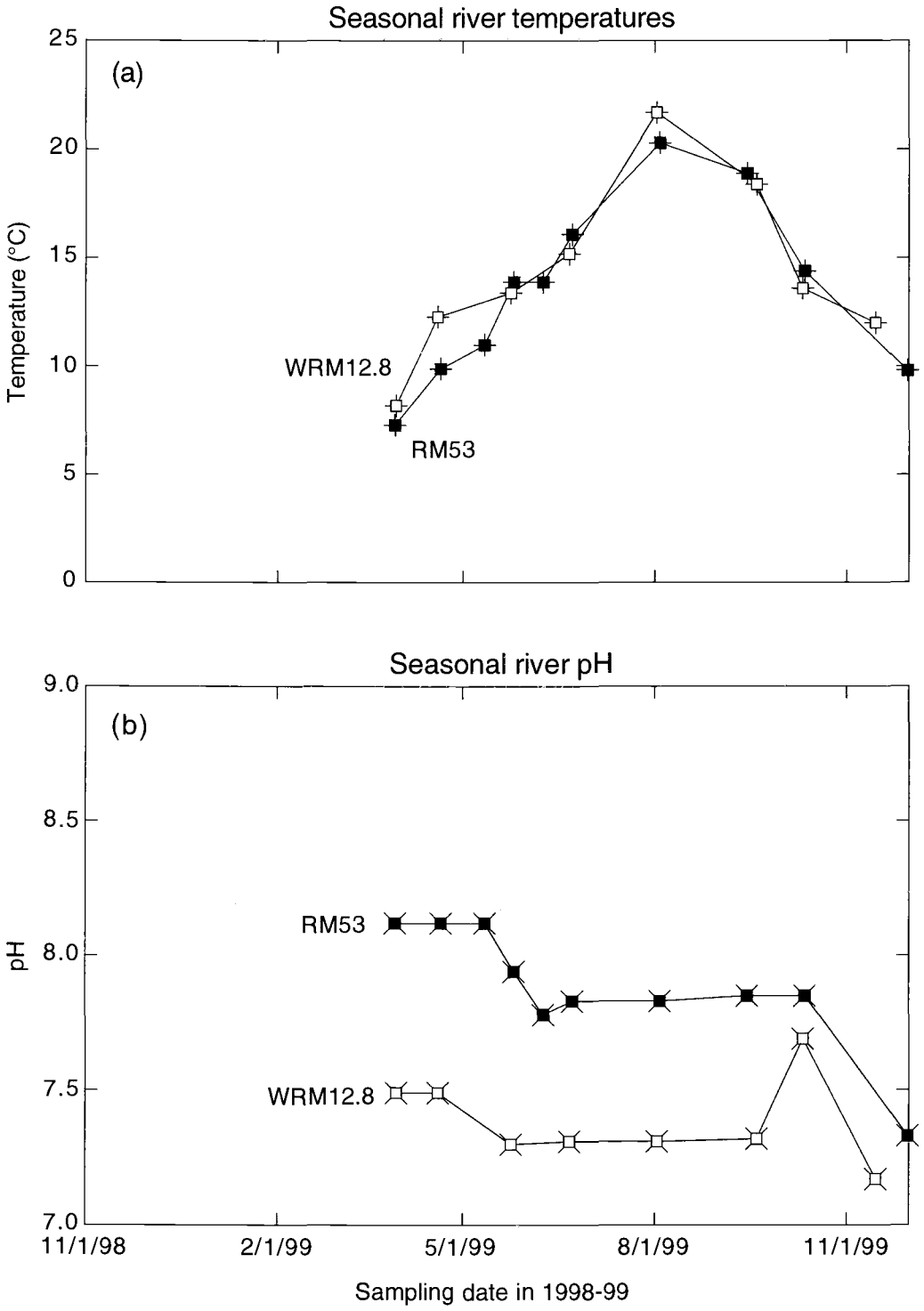

Fig. 3.3: (a) River temperature during 1999. (b) Riverwater pH during 1999.

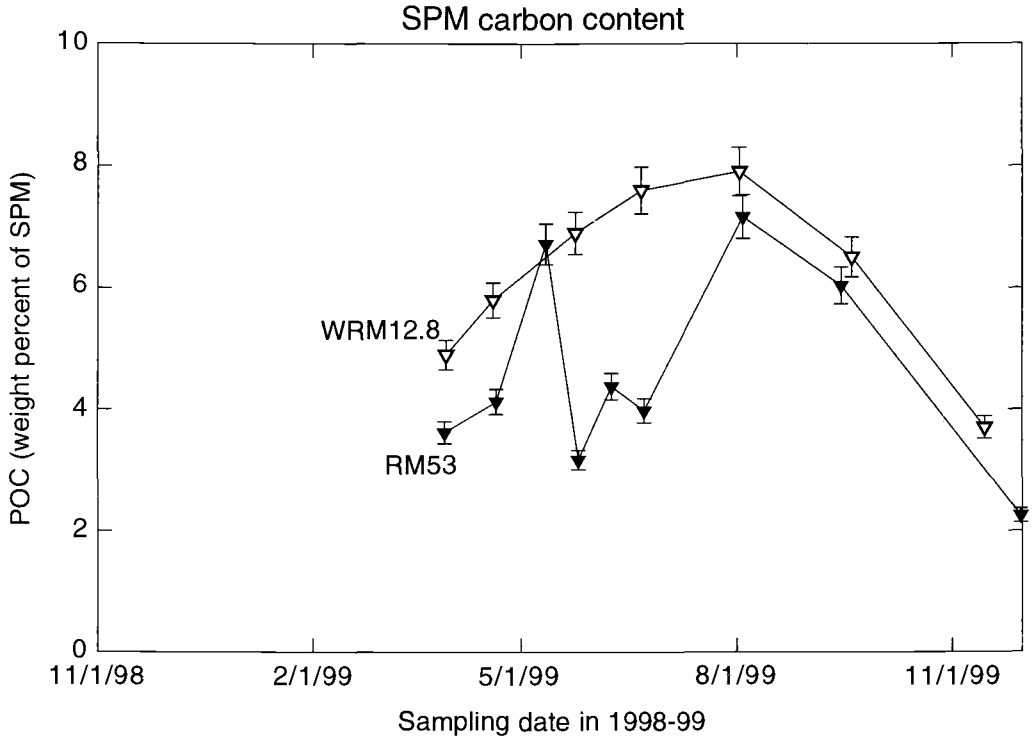

Fig. 3.4: (a) Particulate organic carbon content of SPM. Error bars represent 1σ standard deviation.

the spring, but declined to low values in mid-summer before being restored to a maximum in August. This pattern in %POC in the Columbia is generally consistent with the effects on SPM of seasonal phytoplankton blooms described by Sullivan (1997) and Sullivan et al. (2001).

One curious feature in the %POC time series in the Columbia is the minimum in late May and June. This minimum is misleading in part due to the normalization of the data. For example, absolute POC concentrations during June in the Columbia were 0.8 - 0.9 mg/L, essentially the same as the 0.82 mg/L POC on May 11 (see Table A.1 in Appendix A); however, SPM concentrations in June were considerably higher in June than on

May 11, thus rendering lower %POC values in June. Throughout the year in both rivers, minima in %POC often correspond with maxima in SPM concentration (Table A.1, Appendix A) and thus are a result of dilution by large amounts of eroded mineral material mobilized by high flows.

Aluminum – Over the course of one year, the weight percent of aluminum in the SPM (Al_{SPM}), varied significantly (Fig. 3.5a), but in opposite direction from %POC (Fig. 3.4a). This was the case in both the Columbia and Willamette rivers. In both rivers, $\%Al_{SPM}$ was least (approximately 7.5-7.8% in the Columbia and 7.9-8.0% in the Willamette) in late spring through late summer.

Another way to look at the aluminum content of SPM is as weight percent of the mineral fraction of SPM (Al_{min}). This is different than looking at Al_{SPM}. A change in Al_{min} signifies a change in the mineral composition or type. If this number remains relatively constant over time, then a change in Al_{SPM} signifies change in the composition of the SPM. The equation used to calculate Al_{min} is as follows:

$$Al_{min} = \frac{Al_{SPM} m_{SPM}}{m_{SPM} - 4.2POC_{SPM}} \qquad \text{(eq. 3-1)}$$

where m_{SPM} and POC_{SPM} are the mass of SPM and the percent particulate organic carbon of SPM, respectively. The term $4.2POC_{SPM}$ in equation 3-1 is equal to the sum of POM and BioSi. Two components of SPM are particulate organic matter and biogenic silica (POM and BioSi) (Prahl et al., 1997). Organic matter is generally twice the mass of POC

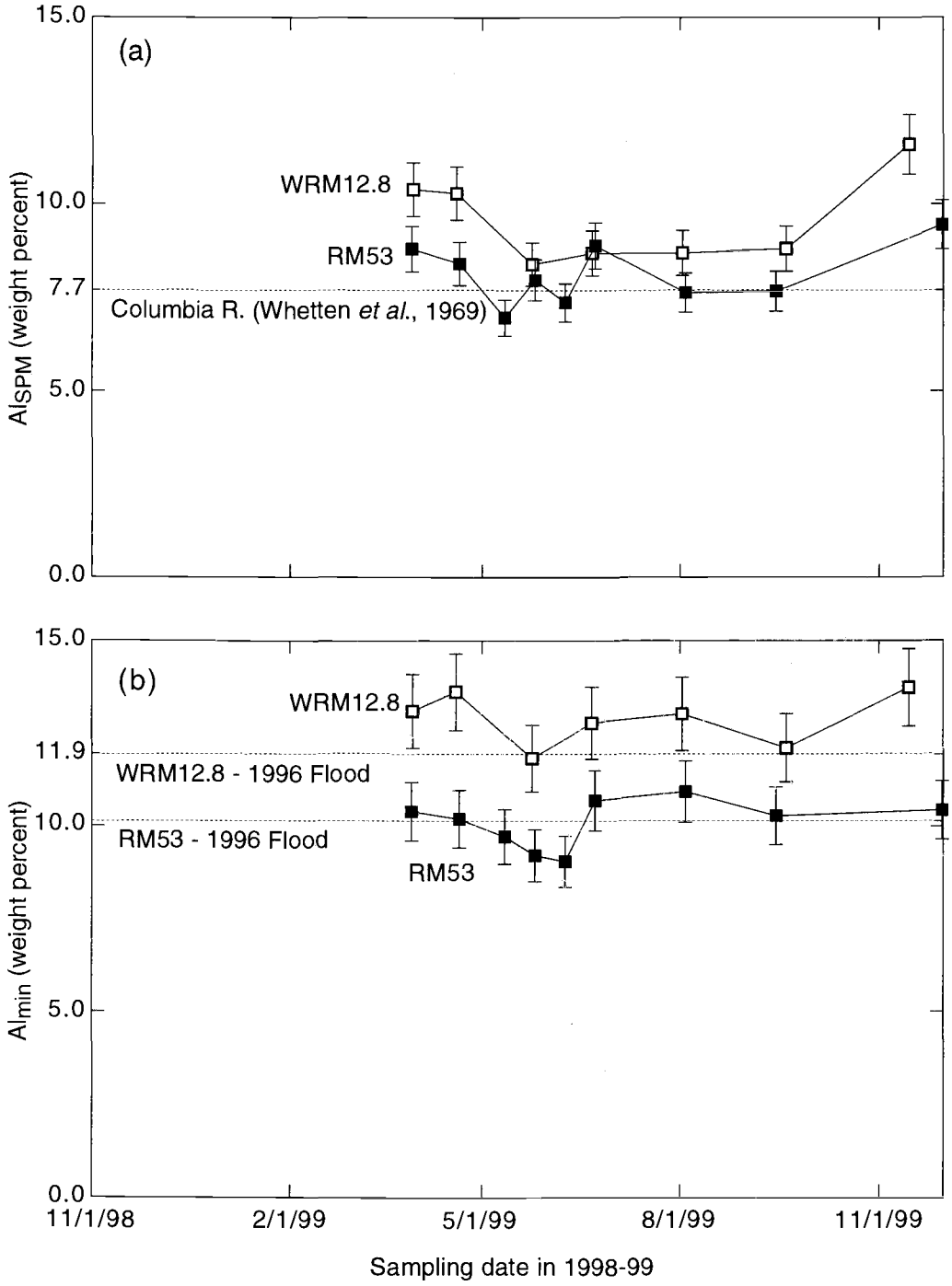

Fig. 3.5: (a) Particulate aluminum measured as weight percent of SPM. Average Al content of Columbia River sediment is 7.7% (Whetten et al., 1969). (b) Approximate concentration of particulate aluminum measured as weight percent of the mineral component of SPM. Dotted lines at 10.1% and 11.9% identify Al content of SPM during the 1996 flood, periods when organic contribution to the total SPM was negligible (Sullivan, 1997; Sullivan et al., 2001). Error bars represent 1σ standard deviation.

(Rashid, 1985), and BioSi content in surface and non-turbid bottom waters in the Columbia River have been observed to be approximately 1.1 times POM (Prahl et al., 1997).

Plotted versus time, Al_{min} looks reasonably constant at approximately 11% by weight in the Columbia over most of the year, and 13-14% by weight in the Willamette (Fig. 3.5b). Supporting the results of these calculations are analyses of SPM collected during the flood event in February 1996. POC contribution to this SPM was negligible, making these samples a good proxy for the mineral component of SPM. Al_{SPM} of these samples was 10.1% in the Columbia and 11.9% in the Willamette (Sullivan, 1997; Sullivan et al., 2001), similar to calculated Al_{min} of SPM collected as part of this thesis.

This similarity of Al_{min} to Al_{SPM} in flood material, coupled with the relative consistancy of Al_{min} throughout 1999 allows us to attribute variability in Mn/Al and Fe/Al to changes in Mn and Fe, rather than variability of Al_{min}.

Manganese and iron – In 1996 the Mn/Al ratio reached a peak in August in both the Columbia and Willamette Rivers (Fig. 3.1). Peak Mn/Al ratios of 0.023 in the Columbia and 0.045 in the Willamette in 1999 (Fig. 3.6a) were slightly less in magnitude than in 1996, and occurred one to two months later. Although the sampling period did not include many of the winter months, the first and last samples of the series (March 29, both rivers, and November 11 and November 29, WRM12.8 and RM53, respectively) are near the Columbia River sediment average of 0.010 (Whetten et al., 1969).

Compared to manganese, the trend for iron in both rivers is relatively invariate. With the exception of one high point on May 11 and one low point on May 25, Fe/Al ratios in Columbia River SPM remained relatively constant at approximately 0.55

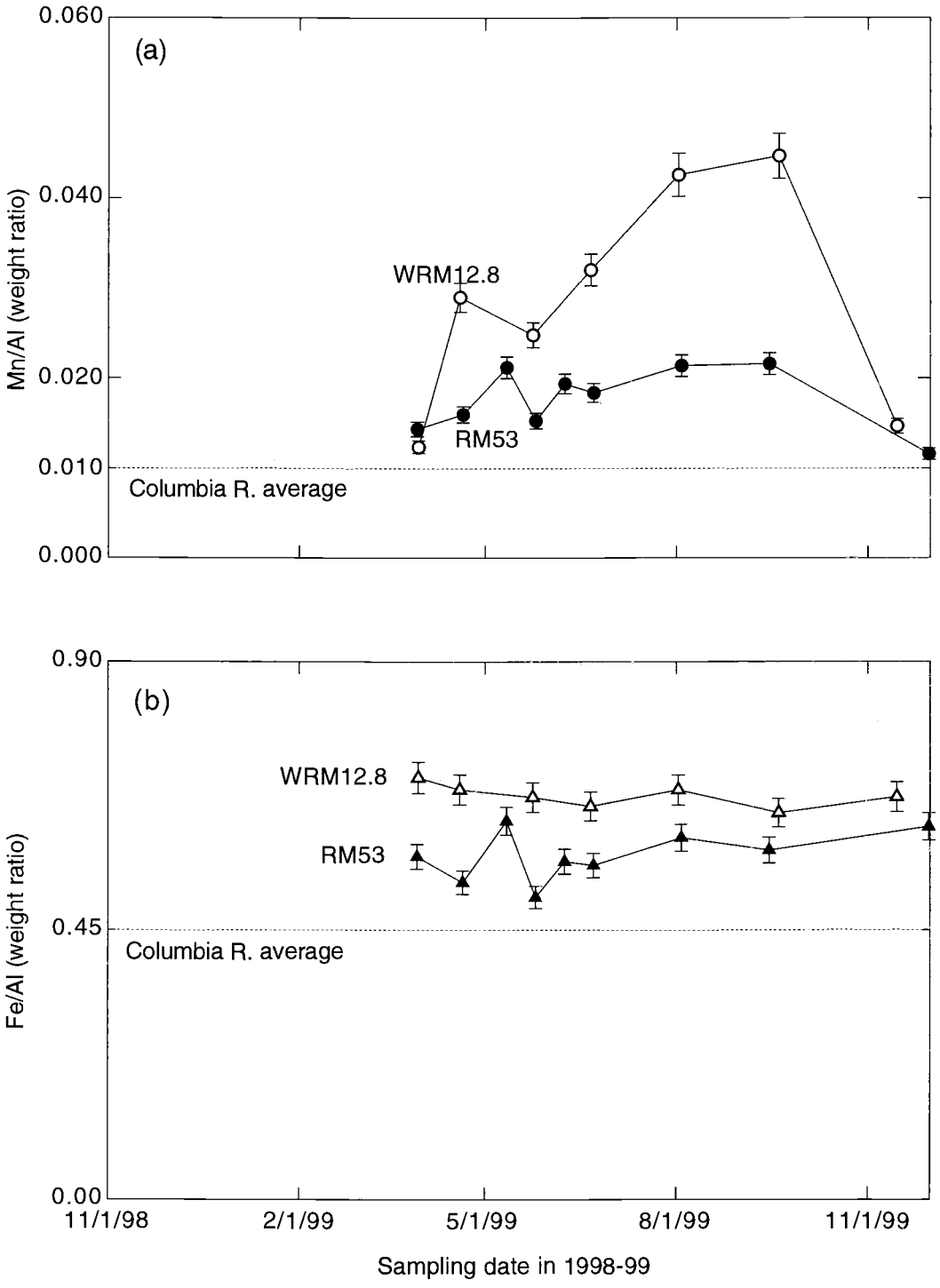

Fig. 3.6: Mn/Al (a) and Fe/Al (b) in SPM. Columbia river sediment averages of the two ratios are 0.01 and 0.45, respectively (Whetten et al., 1969). Error bars represent 1σ standard deviation.

throughout 1999. Willamette River SPM varied in Fe concentrations even less, maintaining a constant value of 0.68 throughout the year.

Elemental Maps – Elemental maps were generated for SPM samples collected in spring, summer and fall of 1997 (97a, 97b, and 97c series, respectively) (Appendix B). Aluminum and silicon elemental maps appear well correlated. Particles with high aluminum contents also have high silicon contents. This was expected and confirms that the SPM analyzed is composed of mostly aluminosilicate clays. Manganese and titanium elemental maps are not correlated with each other or with the aluminum and silicon maps (see Fig 3.9 and Appendix B). Bright spots indicating high concentrations of Mn or Ti appear either in "holes" on the aluminum map or in locations where the relative aluminum contents were low.

3.3 Seasonal variability of Mn and Fe

Compositional data from RM53 produced by the U.S. Geological Survey (USGS), when combined with data collected as part of this thesis, data from Sullivan (1997), and LMER data, comprise a reasonable time series spanning several years (Fig. 3.7). An annual pattern of seasonal variability in Mn/Al in the Columbia River begins to form.

Seasonality in particulate iron and manganese concentrations has been observed in other fluvial systems. In the St. Lawrence River, particulate Mn concentrations varied from 0.8 mg/g SPM in the winter to 1.8 mg/g SPM in the summer during 1983 and 1984 (Cossa et al., 1990). These are almost identical to the concentrations of 1.0 mg/g SPM in the winter and 1.5 mg/g SPM in the summer observed in the Columbia River (Table A.1).

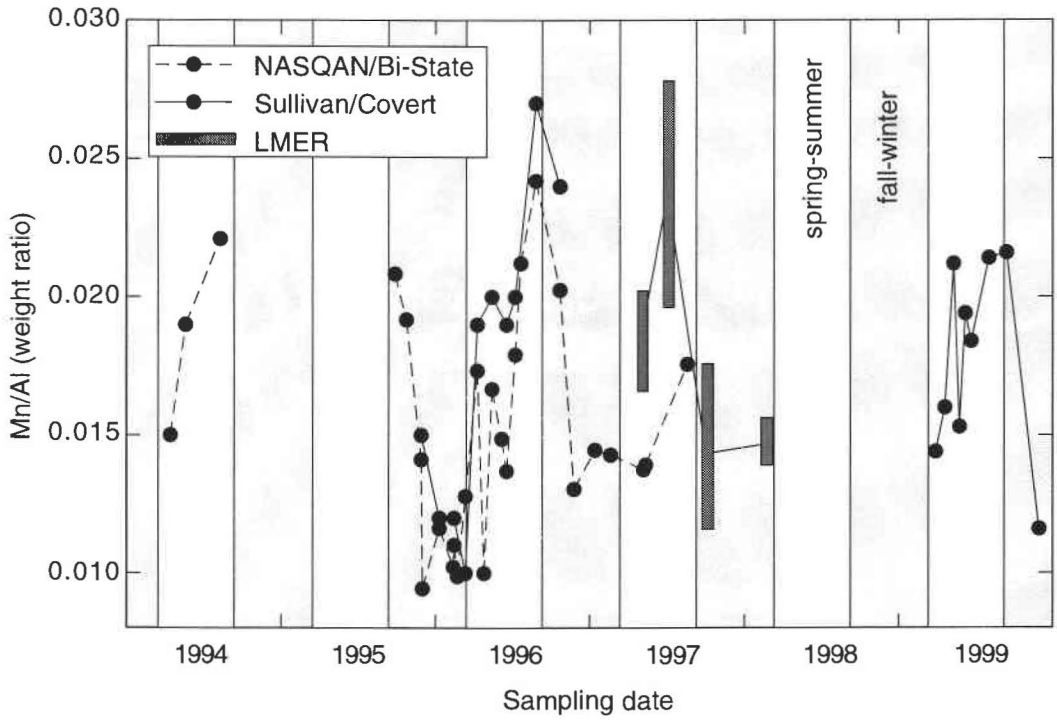

Fig. 3.7: Compilation of all Mn/Al data at RM53. Compiled from data collected as part of the USGS NASQAN and Bi-State programs, from Sullivan (1997), and the present study. Shading emphasizes the seasonality of Mn/Al.

The inverse periodicity is observed for dissolved Mn in the St. Lawrence, with maximum concentration in the winter and spring (8.5 ± 2.1 μg/L and 10.0 ± 6.1 μg/L, respectively), and minimum in the summer (1.8 ± 1.4 μg/L) (Cossa et al., 1990). However, this relationship does not imply a cause and effect link.

An investigation of Mn and Fe seasonality in the Kalix River in northern Sweden provides a better case for a link between particulate and dissolved Mn (Pontér et al., 1990; 1992). Like the Columbia, Willamette, and St. Lawrence rivers, seasonal variation in particulate Mn is observed (Fig. 3.8), albeit on a much larger scale (Mn/Al ranges from 0.1 to >0.4 in the Kalix versus 0.01 to >0.04 in the Columbia and Willamette). And, like the St. Lawrence, dissolved and particulate Mn show a rough inverse relationship. The relation-

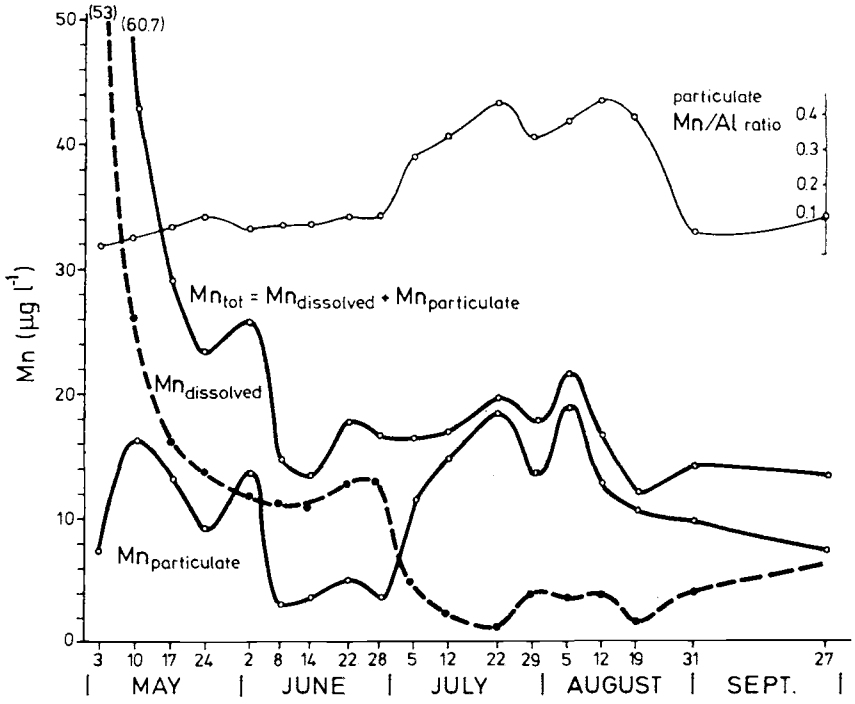

Fig. 3.8: Dissolved and particulate manganese in the Kalix River during 1982. (Adapted from Pontér et al., 1990)

ship between dissolved and solid Mn is better, however, when dissolved Mn is compared to particulate Mn/Al.

Although dissolved Mn data were not collected as part of this thesis, observations of similar dissolved Mn behavior in the St. Lawrence and Kalix Rivers, and also the Mississippi (Shiller, 1997) show that this is a widespread behavior. Therefore, it is highly likely that dissolved Mn in the Columbia and Willamette rivers also varies on a seasonal basis.

3.4 What is the form of "excess" Mn in the Columbia and Willamette Rivers?

The mirror image quality of particulate Mn/Al and dissolved Mn in the Kalix river (Fig. 3.8) implies a conversion from dissolved to solid phase. The easiest way to achieve this is via an oxidation of Mn^{II} to $Mn^{III,IV}$ and precipitation of the oxides. If this process

were occurring in the Willamette and Columbia rivers, we would expect to see Mn-oxides in SPM samples. Two paths of investigation offer strong support for the hypothesis that "excess" manganese in SPM exists in the oxide form. Furthermore, it appears that the oxides exist as discrete "micro-nodules," a form of Mn-oxide found in bottom sediments in the St. Lawrence estuary (Sundby et al., 1981), rather than as oxide coatings precipitated on aluminosilicate clays.

Elemental maps of samples collected at RM53 in the spring, summer, and fall (97aU2105M, 97bU1125M, and 97cU1109M, respectively) show the physical distribution of individual elements within SPM (Fig. 3.9). Individual clay particles are well resolved by the aluminum maps. In contrast, the Mn maps do not reveal an image similar to the aluminum map. In general, bright spots on the Mn maps do not coincide with the clay particles, an observation interpreted to mean that high concentrations of Mn in SPM exist separately from the clay minerals.

The magnitude of Mn/Al seems to have no relation to the population of small, Mn-rich particles seen in the elemental maps. It was expected that more bright spots indicating high Mn content would be seen in photos of 97aU2105M than in either 97bU1125M or 97cU1109M, given respective Mn/Al measures of 0.032, 0.017, and 0.010. This is not the case. One possible source for the discrepancy is the heterogeneous nature of the samples. Subsamples of the total SPM collected were extracted for analysis with SEM. After these subsamples were extracted, the remaining sample was homogenized with a ball mill and analyzed for metal content. As a result, the samples examined via SEM may not accurately represent the bulk sample.

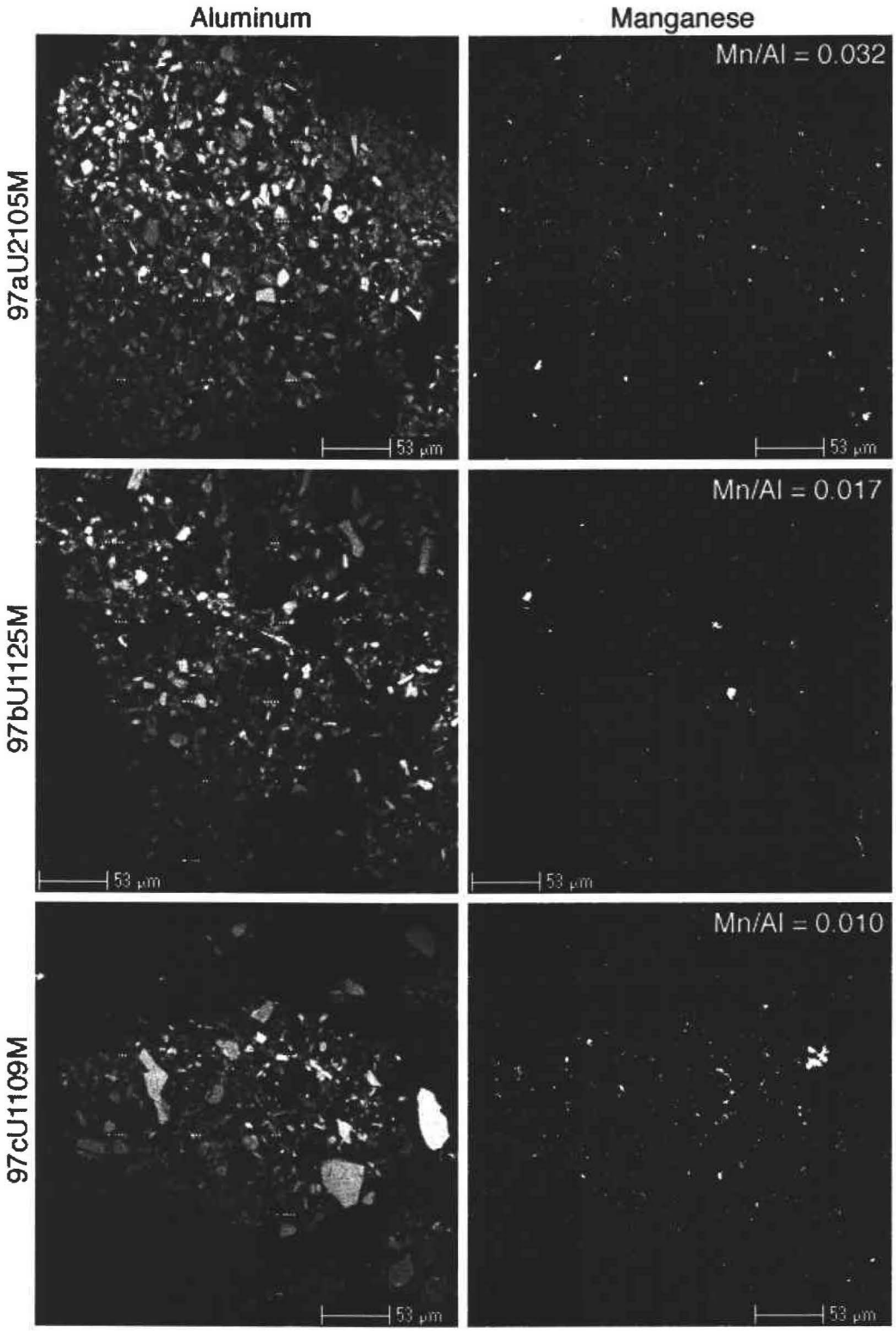

Fig. 3.9: Elemental maps of three SPM samples collected at RM53 and processed via ultrafiltration. Mn/Al of the samples was determined with ICP-AES.

Despite this possible error introduced by sub-sampling, conclusions with respect to the distribution of Mn in SPM can still be made. It is more likely that the areas of concentrated Mn are oxides. Additionally, the locations of high Mn content are all much smaller than the clay particles shown in the Al map, leading to the belief that "excess" Mn exists as small, discrete, oxide particles. Similar conclusions are obtained via Owen Tube settling experiments.

The use of Owen Tubes to separate SPM on the basis of settling velocity has aided the investigation of the form of "excess" Mn. A more thorough discussion of this technique and results of the experiments can be found in chapter 4. By using Owen Tubes to capture sediment as a function of settling velocity, it was seen that the slowest settling particles of SPM, those with settling velocities less than 0.011 cm/s, had the highest Mn concentrations. The average ratio of Mn to Al in these particles was 0.036, more than three times the crustal average of 0.011. Three other settling velocity ranges were collected: 0.011 to 0.044 cm/s, 0.044 to 0.22 cm/s, and > 0.22 cm/s. Average Mn/Al for each of these fractions was 0.018, 0.017, and 0.016 cm/s, respectively. The distribution of clay particles, approximated by the distribution of weight percent aluminum, does not show this preference for the slow settling fraction. This is evidence that aluminosilicate clays and manganese-rich particles are not the same particles, ruling out the possibility that the "excess" manganese exists as a coating on clay particles. The alternative is that the Mn-rich particles are discrete.

Although there is no direct evidence (for example, by x-ray diffraction or analysis of selectively leached oxide phases) for "excess" manganese existing as small, discrete,

oxide particles, results from Owen Tube experiments and visual analysis by SEM lead us to believe that "excess" Mn does occur in this form.

3.5 Summary

1. Seasonal variability of Mn/Al observed by Sullivan in 1995-6 was confirmed in 1999, indicating that the earlier observation was not an artifact of an unusual water year. Data obtained from the USGS for intermediate years improved the confirmation. Seasonality in Mn/Al is a feature that is also found in other river systems, such as the St. Lawrence and Kalix, and is perhaps tied to seasonalities in dissolved Mn, such as those observed in the Kalix and Mississippi Rivers, although the link has not been rigorously tested.

2. Electron microprobe was used to generate elemental maps of Columbia River SPM. From these maps, it appears that Mn-rich particles are separate from the aluminosilicate-type particles, a result confirmed by particle settling experiments (see Ch. 4) . Reports of mirror image Mn/Al and dissolved Mn variation imply an oxidation and precipitation of dissolved Mn, leading us to believe that the discrete Mn-rich particles seen in Columbia and Willamette river SPM are Mn-oxides.

4: EFFECTS OF PARTICLE SETTLING ON SPM COMPOSITION

4.1 Introduction

It is documented that seasonal variability in riverine primary production results in a seasonal variability in the organic composition of SPM (Pocklington and Tan, 1987; Sullivan, 1997; Sullivan et al., 2001). Additionally, seasonal variation in the inorganic components (e.g. Mn and Fe) of SPM has been observed (Cossa et al., 1990; Pontér et al., 1990, 1992; Canfield, 1997; Ch. 3, this thesis). Here, compositional variability in SPM that takes place over much shorter time periods is reported. This short-term variation is superimposed on the seasonal signal and is observable over several hours rather than months. In some cases, the magnitude of variation seen over several seasons is large enough that variability over short time frames is swamped by the seasonal signal. In other cases, the short term variation is large enough that its effects can be clearly seen superimposed on the seasonal signal, highlighting the importance of taking this variation into account when discussing magnitudes of seasonal variation.

The work presented in this chapter is guided by the hypothesis that the short-term variability in SPM concentration and composition is largely driven by tidally mediated settling and resuspension processes. Water flow in the Columbia River (below the Bonneville dam, including RM53), which over short time scales (<24 hrs) is mostly governed by tidal forces, promotes alternating particle settling and resuspension processes. During particle settling, the more dense particles settle faster, while the less dense particles settle slower, or perhaps remain in suspension. It is reasonable to expect that the effect of this

process would be a separation of particles with different biogeochemistries, which likely span a range of densities and sizes.

Recently, short-term variability in SPM concentrations in the tidal freshwater stretch of the Seine has been quantified (Guézennec et al., 1999). Elsewhere, investigations have measured chemical differences between slow and fast settling particles (e.g. Niedergesäss et al., 1986; 1987; Williams and Millward, 1998). For example, at an upriver site in the Elbe River in Germany (Niedergesäss et al., 1986; 1987), settling velocities of Al are approximately 3-10 times that of average SPM, while Mn settles from approximately 1 to 7 times SPM settling rates, and Fe settling rates are approximately 0.4 times the mean SPM settling rates. At downstream, tidally influenced sections of the river, metal distributions within the SPM are significantly different from the upriver case. Here, Al, Fe, and Mn all settle slower than the mean settling rate of SPM.

While separate investigations have observed tidally variable SPM concentrations in river water, and others have shown biogeochemical differences among particle populations with different settling velocities, the two have yet to be linked. The evidence presented here provides this link by describing SPM concentration and composition at RM53 as a function of both tidally modulated river velocity and settling velocity.

4.2 Results

Twelve hour time series at RM53 – The LMER cruises in spring, summer, and fall of 1997, and winter of 1998, allowed for sample collection from mid-depth in the river every couple of hours at the same location for 12-hour periods. In order to preserve a sense of continuity and consistency, the results of these samplings are first displayed with the time-

axis spanning one year to highlight the seasonal variability (Fig. 4.1). The vertical bars in the Mn/Al, Fe/Al, %POC, and Chl *a*/POC plots indicate the range of values measured during each 12-hour series. The range indicated by these bars is large (significantly greater than 1σ analytical uncertainties), yet the averages of the ranges are consistent with seasonal variabilities already described at RM53. Suspended loads are highest in spring and fall, and lower in summer and winter; Mn/Al and Fe/Al follow the seasonal periodicities described in chapter 3; and %POC and Chl *a*/POC are consistent with findings by Sullivan et al. (2001). However, if you reduce span of the time-axis from one year to 12 hours, each of these 12-hour time-series displays a variability that appears to follow a periodic pattern.

Water flow at RM53 during each time series (unpublished data, Portland USGS) is plotted alongside SPM concentration and composition (Figs. 4.2; 4.3; 4.4). In all cases the flow varies as a result of flooding and ebbing Pacific tides. Tidal effects on river flow are significant at times, reducing flows to less than 5,000 m^3/s during the 97bU11 and 97cU11 time series (Figs. 4.3 and 4.4), and reversing the river flow for a short period during the 97cU11 time series. It is important to note that these river flows represent the average flow accross the channel and are based on river velocities measured by the USGS on the north side of the Columbia River channel at RM53, opposite the sampling location at RM53. Actual river flows at the sampling location will not necessarily match those plotted. However, the USGS flows are useful in providing a tidal reference point to which SPM concentration and composition may be compared.

In early May, SPM concentrations ranged from approximately 26 to 40 mg/L (Fig. 4.2a). It appears that this variability is coupled to the water flow, as lowest SPM concen-

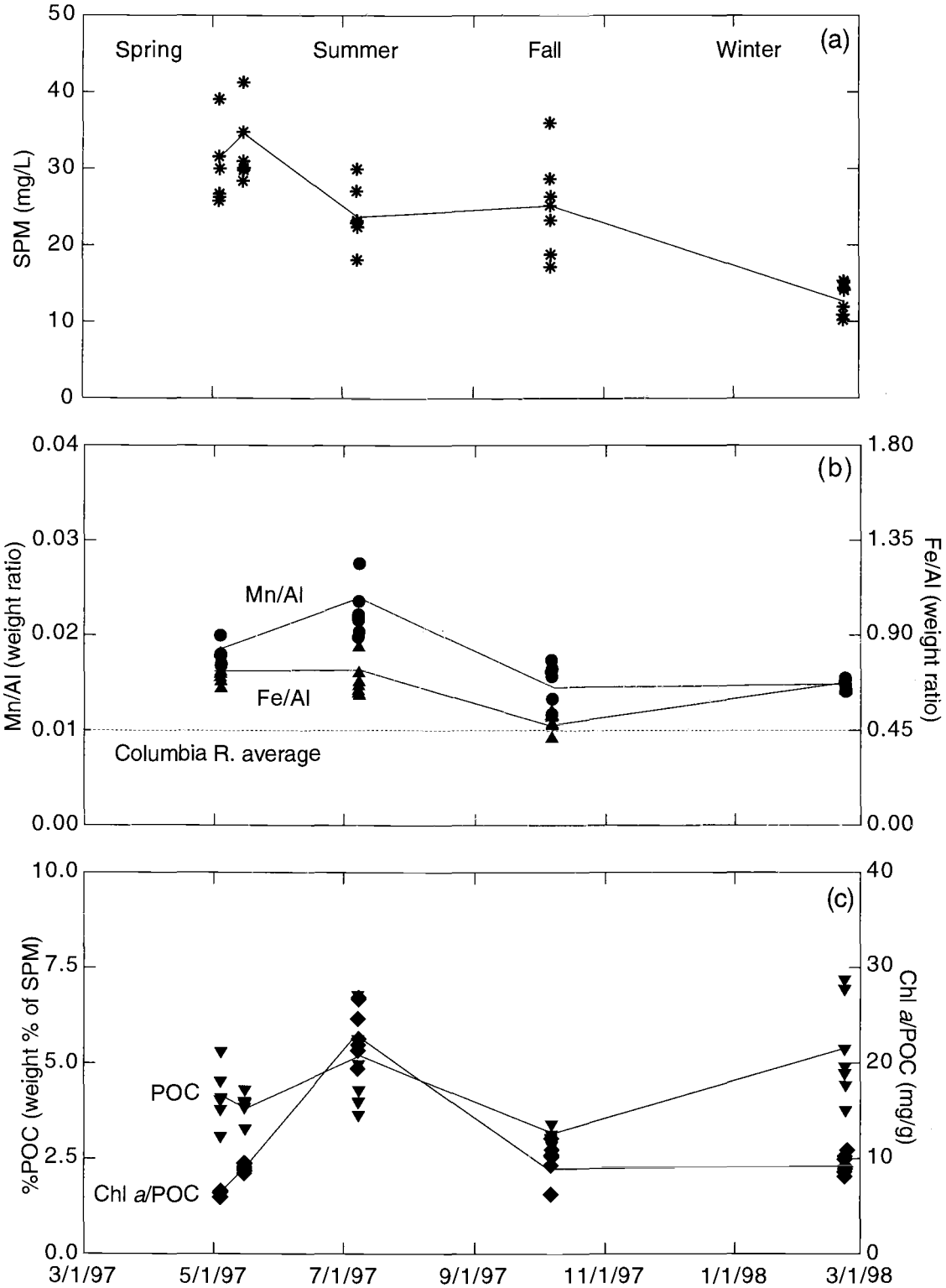

Fig. 4.1: Variability in SPM concentration in 1997 is shown along with several indicators of SPM particle quality.

trations occur during or shortly after greatest flows, while higher SPM concentrations occur during low flow periods. Particulate manganese and iron show little variability (in terms of Mn/Al and Fe/Al) over the 12-hour period captured by the 97aU11 time series (Fig. 4.2b). Average values of Mn/Al and Fe/Al during this period are 0.018 and 0.71, respectively, both of which are nearly double average Columbia River sediment values of 0.010 and 0.45 (Whetten et al., 1969), respectively. The particulate organic carbon content of SPM in May (Fig. 4.2c) was inversely related to SPM concentration (Fig. 4.2a), and varied from 3.1 to 5.3 percent by weight. Chl *a*/POC during this 12-hour period was nearly constant at 6.5 mg/g, a level indicative of carbon that is below that of healthy phytoplankton (Meybeck et al., 1988), indicating significant detrital contribution.

Several changes in the SPM were apparent by early July (Fig. 4.3). Average SPM concentrations were 6 mg/L lower than two months earlier. Also, the the inverse relationship of SPM to flow seen in early May is not apparent here (such a relationship may be evident if longer time series were collected). The largest differences between May and July are in Mn/Al and Chl *a*/POC variability. Particulate Mn/Al levels ranged from 0.020 to 0.028, significantly greater than in May. Undoubtedly a spring phytoplankton bloom occurred to increase Chl *a*/POC from 6.5 mg/g in May to 19.4 - 27.0, indicating large algal contribution to the total POC. In contrast, the behavior of particulate Fe/Al and %POC were very similar to the behaviors in May. In addition to generally greater levels of Mn/Al and Chl *a*/POC, these two parameters tend to vary in a periodic manner that appears to be the inverse of the periodicity of flow, %POC, and perhaps SPM concentration.

In the fall (October 6, Fig. 4.4) and winter (February 21-22, Fig. 4.5) the components of SPM behaved much as they did in the early spring. A slight variability in Mn/Al

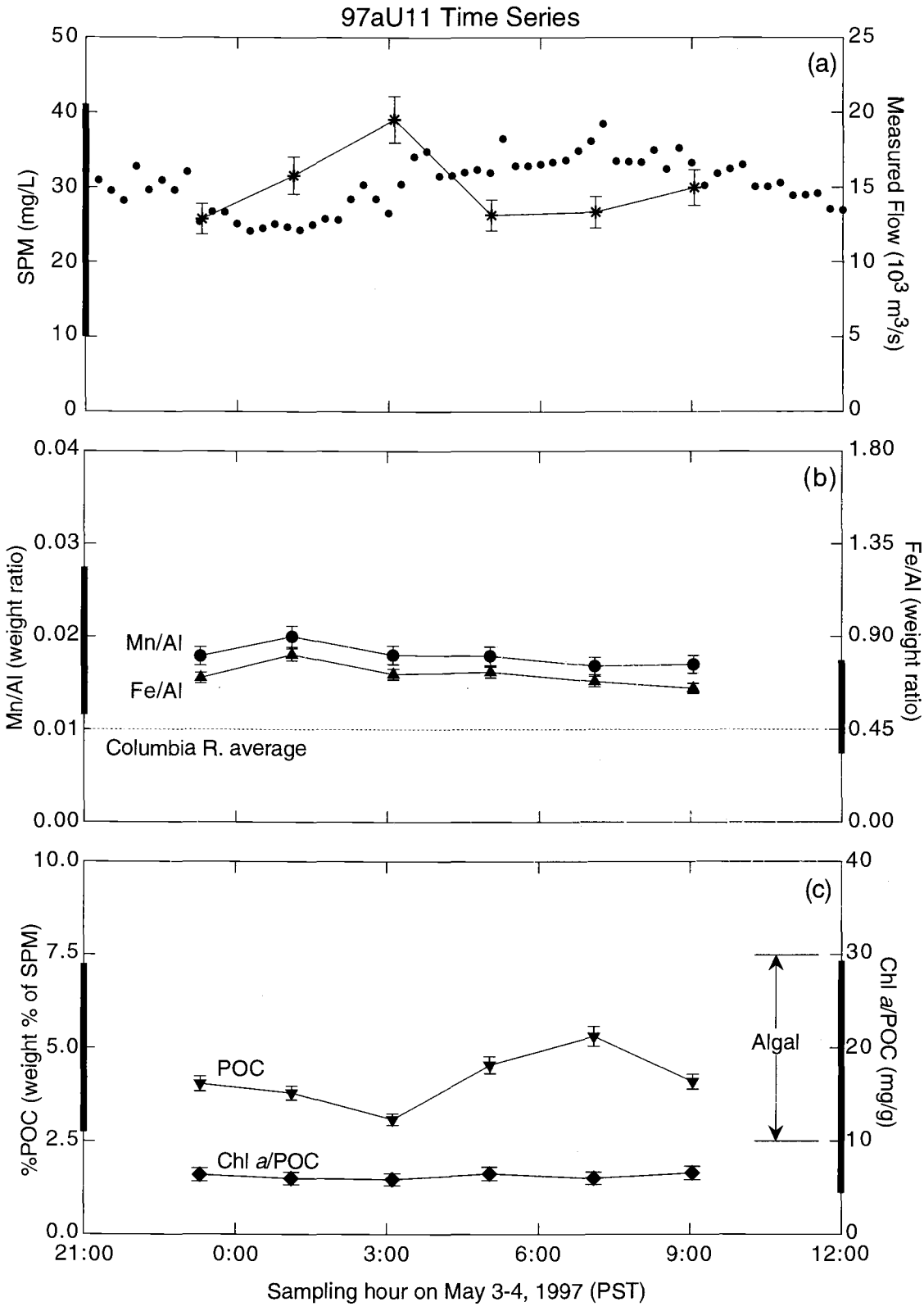

Fig. 4.2: Twelve hour variability of SPM concentration (a), metal characteristics (b), and organic characteristics (c). Bold lines on the y-axes indicate seasonal range observed and shown in Fig. 4.1.

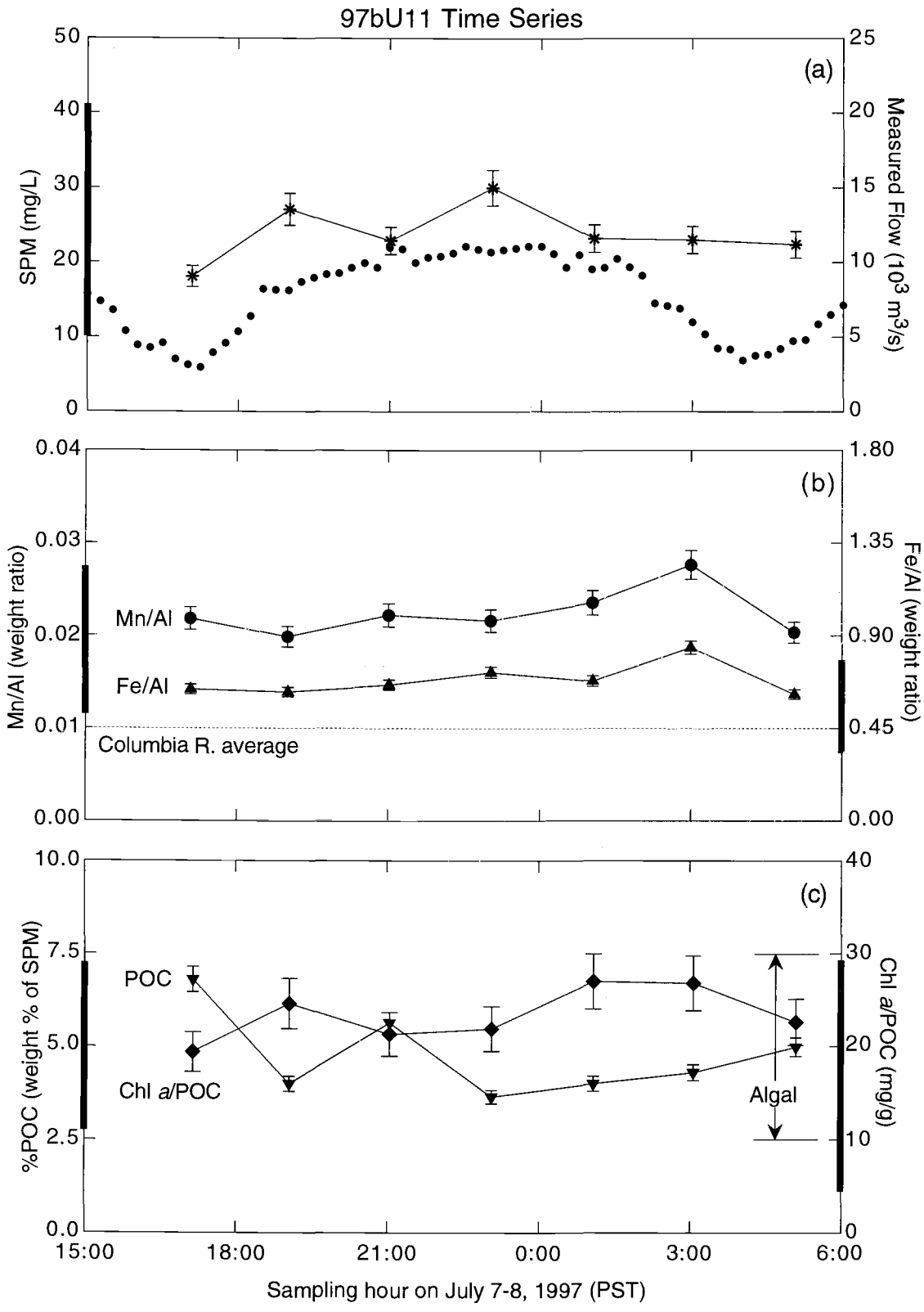

Fig. 4.3: Twelve hour variability of SPM concentration (a), metal characteristics (b), and organic characteristics (c). Bold lines on the y-axes indicate seasonal range observed.

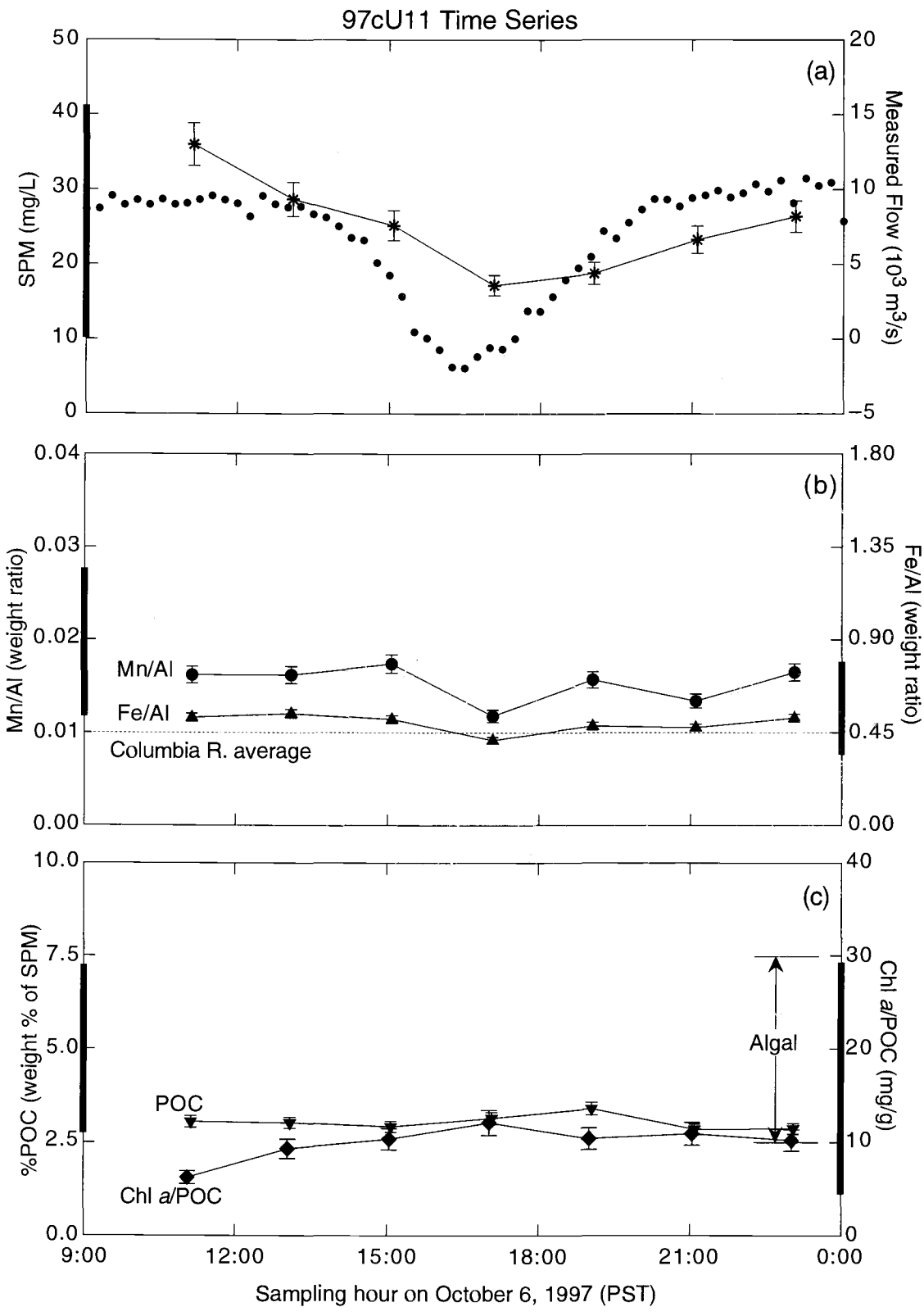

Fig. 4.4: Twelve hour variability of SPM concentration (a), metal characteristics (b), and organic characteristics (c). Bold lines on the y-axes indicate seasonal range observed.

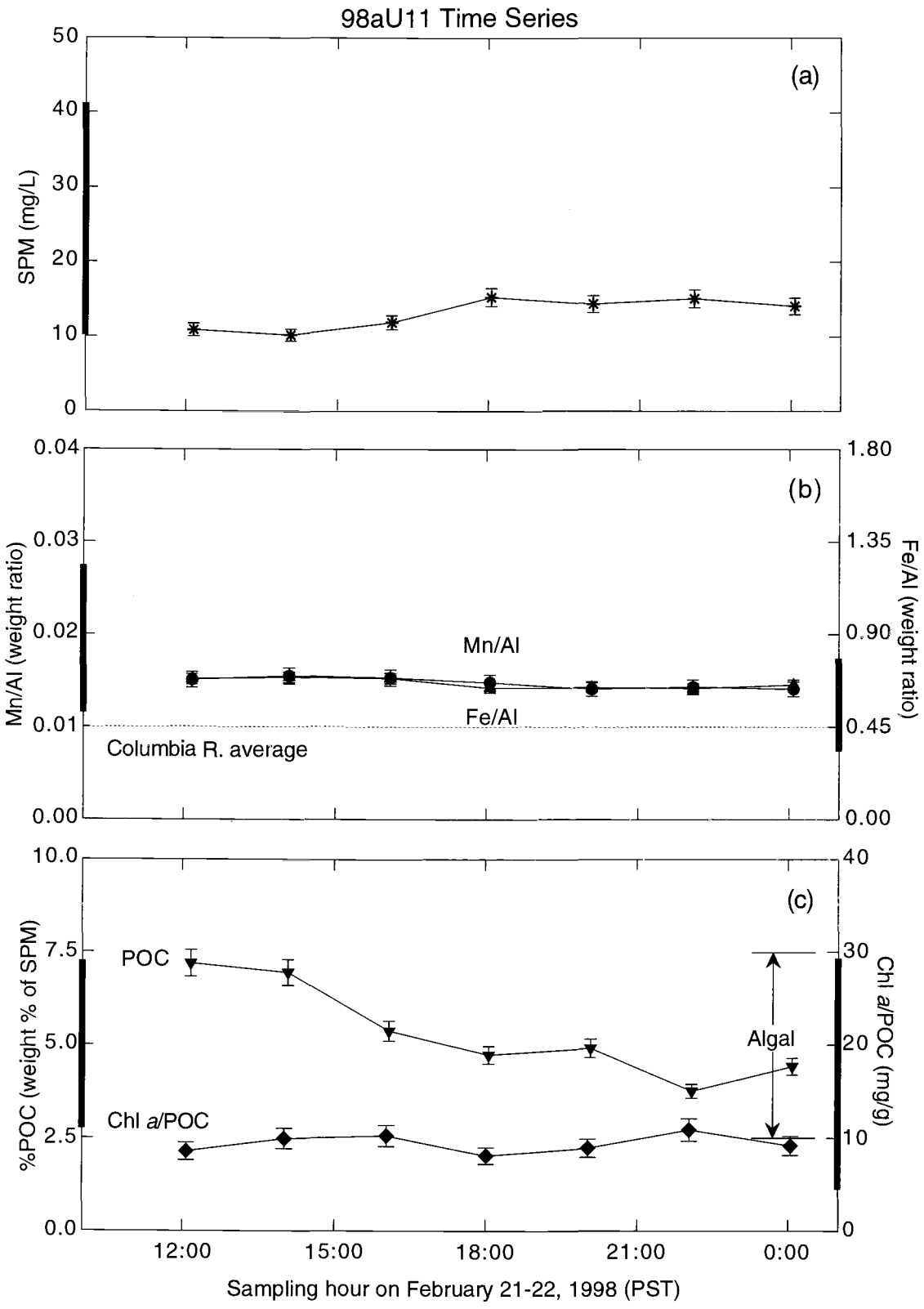

Fig. 4.5: Twelve hour variability of SPM concentration (a), metal characteristics (b), and organic characteristics (c). Bold lines on the y-axes indicate seasonal range observed.

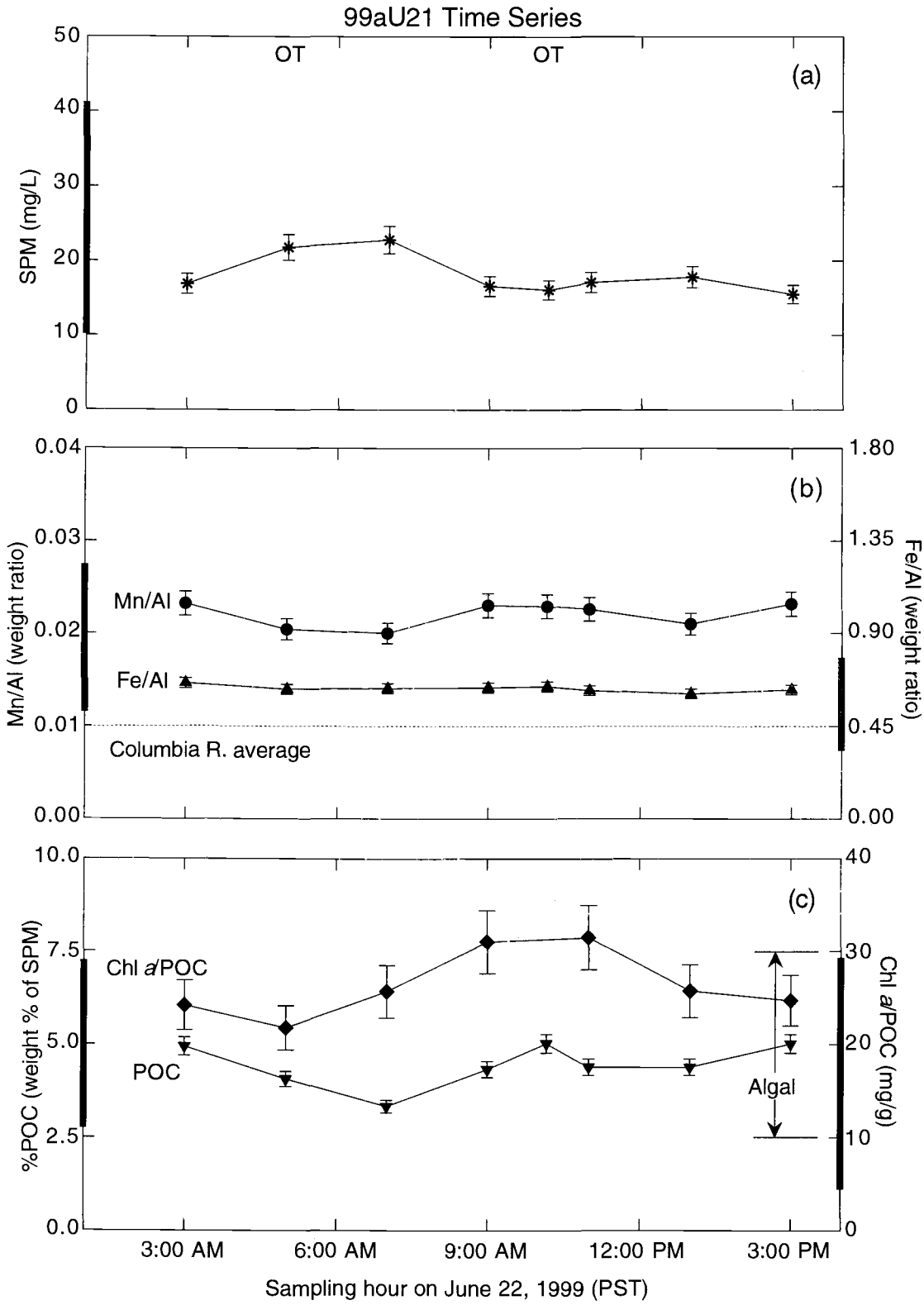

Fig. 4.6: Twelve hour variability of SPM concentration (a), metal characteristics (b), and organic characteristics (c). Bold lines on the y-axes indicate seasonal range observed in 1997. "OT" marks the times the samples were also collected and processed with Owen Tubes.

and Fe/Al was seen in October, but was noticably absent in February. Chl *a*/POC ratios which were high in summer had returned to the low levels seen in spring. One striking difference between fall and winter, however, is the behavior of %POC. In the fall, %POC was constant over 12 hours at around 3% of the SPM (Fig. 4.4c). In the winter, %POC ranged from around 3.5% to 7.5%.

A year and a half later, in July 1999, a 12-hour time-series (Fig. 4.6) was conducted along with Owen Tube settling experiments. As expected, variability in the geochemical properties of the particles was similar to the variability seen in June 1997.

Owen tube settling experiments – Suspended material separated using Owen settling tubes was analyzed for POC, PON, Chl *a*, and metal content (Table 4.1). Since each of the fractions extracted from the Owen Tube contains a mixture of fast and slow settling particles, the data were subjected to a mathematical algorithm used to extract the chemical composition data as a function of settling velocity (refer to Ch. 2). Separation of SPM in this manner reveals a lot about how material is distributed throughout the SPM field.

In general, %POC is greatest in the slowest settling fractions (<0.011 cm/s), though occasionally there is a significant percentage of POC in the fastest settling fraction (>0.22 cm/s) as well (Fig. 4.7a). Given that organic matter is approximately twice the mass of carbon (e.g. Ertel and Hedges, 1984), we can assume that most of the organic matter is associated with the slowest settling fractions, with some concentration in the faster settling material.

An examination of chlorophyll content in the various settling classes of SPM helps explain the %POC distribution (Fig. 4.7b). In all cases Chl *a*/POC, an indicator of the

Table 4.1: Concentrations and composition of SPM collected at RM53. Both fractions drawn directly from the Owen Tube and settling rate fractions are shown.

	Owen Tube Bottle Fractions							Settling Rate Fractions						
Station	Fract.	SPM (mg/L)	POC (wt %)	Al (wt %)	Chl *a* POC (mg/g)	Mn/Al (wt:wt)	Fe/Al (wt:wt)	Settling Fraction (cm/s)	SPM (mg/L)	POC (wt %)	Al (wt %)	Chl *a* POC (mg/g)	Mn/Al (wt:wt)	Fe/Al (wt:wt)
96U1121M	1	86.5	5.2	7.4	4.4	0.017	–							
	2	75.0	3.6	7.8	7.1	0.017	–	$\infty \rightarrow .22$	6.9	6.2	6.6	1.2	0.021	–
	3	45.0	3.2	7.1	11.8	0.017	–							
	4	19.7	5.3	6.3	13.6	0.022	–	$.22 \rightarrow .044$	11.8	1.6	7.8	7.1	0.014	–
	5&6	13.8	6.7	7.6	14.5	0.020	–	$.044 \rightarrow .011$	0.7	7.1	5.6	4.4	0.029	–
	7&8	12.6	6.7	7.5	19.0	0.021	–	$.011 \rightarrow 0$	12.7	6.7	7.7	15.3	0.021	–
99aU1109M	1&2	66.0	2.4	7.9	17.1	0.017	0.61	$\infty \rightarrow .22$	9.7	1.9	8.5	–	0.015	0.58
	3&4	22.7	3.4	7.2	29.7	0.021	0.66	$.22 \rightarrow .044$	6.5	1.6	6.4	–	0.014	0.66
	5&6	10.0	5.7	7.3	29.1	0.028	0.71	$.044 \rightarrow .011$	2.5	2.6	11.0	–	0.017	0.44
	7&8	3.4	10.5	8.1	51.6	0.044	1.06	$.011 \rightarrow 0$	5.7	7.7	6.3	–	0.039	0.95
99aU1121M	1&2	44.7	3.5	6.9	12.4	0.023	0.70	$\infty \rightarrow .22$	7.8	2.9	6.7	2.1	0.020	0.67
	3&4	12.0	5.3	6.5	26.6	0.030	0.78	$.22 \rightarrow .044$	0.5	1.9	42.2	120.0	0.023	0.58
	5&6	11.3	5.5	3.4	23.7	0.039	1.04	$.044 \rightarrow .011$	0.9	3.2	8.0	14.0	0.017	0.50
	7&8	6.9	6.6	3.8	29.9	0.044	1.09	$.011 \rightarrow 0$	8.9	6.0	3.2	26.3	0.045	1.14
99aU2105M	1&2	113.3	2.3	8.9	9.4	0.012	0.50	$\infty \rightarrow .22$	15.4	2.2	9.7	3.8	0.011	0.48
	3&4	34.7	2.8	7.1	19.0	0.016	0.56	$.22 \rightarrow .044$	10.7	1.2	7.7	1.4	0.012	0.54
	5&6	13.3	5.5	7.7	26.2	0.021	0.57	$.044 \rightarrow .011$	2.8	2.3	3.2	3.3	0.017	0.56
	7&8	6.7	8.9	10.5	25.7	0.023	0.60	$.011 \rightarrow 0$	9.2	6.9	9.0	27.6	0.022	0.59
99aU2115M	1&2	92.7	2.4	7.7	9.9	0.016	0.60	$\infty \rightarrow .22$	15.4	1.8	8.5	1.4	0.015	0.57
	3&4	17.3	5.2	5.4	22.6	0.025	0.79	$.22 \rightarrow .044$	4.7	1.8	4.7	11.1	0.021	0.62
	5&6	9.3	7.8	5.0	23.9	0.032	1.03	$.044 \rightarrow .011$	0.4	8.9	55.1	37.1	0.014	0.59
	7&8	8.7	7.8	1.9	24.0	0.058	1.59	$.011 \rightarrow 0$	8.7	7.9	2.3	23.8	0.053	1.47

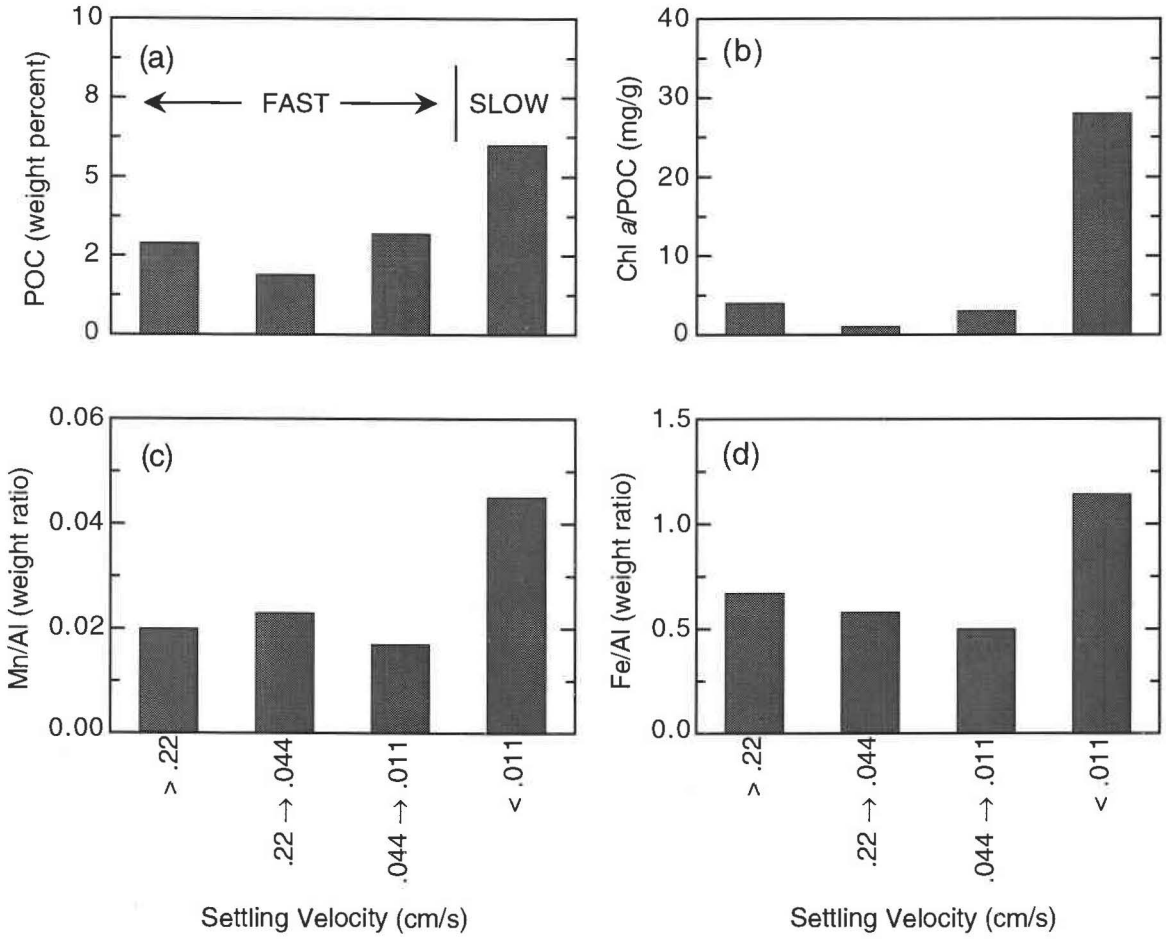

Fig. 4.7: Representative distributions of (a) %POC, (b) Chl *a*/POC, (c) Mn/Al, and (d) Fe/Al across the different settling velocity particles. All the data shown here are from the 99aU1121M Owen Tube, except for Chl a/POC, which is from 99aU2105M.

quality of the carbon, of particles settling slower than 0.011 cm/s was typical of healthy phytoplankton (10-30 mg/g, e.g. Meybeck et al., 1988). In two cases, Chl *a*/POC are anomalously high (120 mg/g, 99aU1121M, 0.22 → 0.044 cm/s, and 37.1 mg/g, 99aU2115, 0.044 → 0.011 cm/s). In both of these cases, however, the percent aluminum measured was also anomalously high (42.2% and 55.1%, respectively), leadingto the conclusion that the numbers obtained for these settling fractions are in error, most likely a result of erroneous mass determinations associated with relatively small mass differences between

unloaded and loaded filters. Neglecting the two erroneous points, Chl *a*/POC was greatest in each of the slowest settling fractions, similar to the distribution of %POC. Unlike the %POC distribution, however, Chl *a*/POC was never large in the fast settling fractions. In fact, Chl *a*/POC averaged only 2.1 mg/g in the fastest settling fractions (Table 4.1). These data are interpreted to mean that the slow settling organic matter in SPM is predominantly phytoplanktonic in origin, while the fast settling organic matter is detrital in nature.

Like the organic components of SPM, metals were not uniformly distributed across the settling fractions. With the exception of the two anomalously high values of Al weight percent mentioned earlier, Al remained between 2.3 and 11 percent by weight, with lower values typically seen in those fractions with high organic contributions to the SPM (Table 4.1). The Mn content of minerals in SPM often was greatest in the slowest settling fraction (Fig. 4.7c). SPM collected at stations 99aU1121M and 99aU2115M had Mn/Al values of 0.045 and 0.053, respectively, in the slowest settling fractions compared to respective averages in the three faster settling fractions of 0.020 and 0.017. Likewise, higher Fe content of SPM was predominantly found in the slower settling fractions (Fig. 4.7d).

4.3 SPM component models

To aid interpretation and discussion of the results, three different component models of SPM are proposed (Fig. 4.8). The first component model divides SPM into three compositional components: mineral, organic, and biogenic silica (Prahl et al., 1997). Partitioning of the SPM in this manner is entirely independant of particle size, settling speeds, or seasonal abundance.

CHEMICAL	SETTLING	TEMPORAL
Mineral • Clays • Autochthonous Fe and Mn oxides **Organic** • Detrital • Mineral associated • Silica associated **Biogenic Silica**	**Slow Settling** • Fe and Mn oxides • Silica • Associated organic matter • Detrital organic matter **Fast Settling** • Clay mineral • Associated organic matter	**Seasonal** • Silica • Mn oxides • Associated organic matter **Year-round** • Clay minerals • Fe oxides • Associated organic matter

Fig. 4.8: Schematic showing the three different component models for SPM. Reorganization of chemical components into settling components is based upon results of Owen Tube settling experiments. Temporal components are based upon seasonal behaviors described in chapter 3 and by Sullivan et al. (2001)

A second way to model SPM is as a combination of components with different settling velocities. In this model the particles are split into two settling classes, fast and slow. Similar models in which sediment is separated into temporarily suspended particulate matter (TSPM) and permanently suspended particulate matter (PSPM) have been used in conjunction with hydrodynamic models to predict trace metal partitioning and distribution in several estuaries in the United Kingdom (Turner, 1996; Liu et al., 1998). For the model in this thesis, the cutoff between fast-settling and slowly- settling particles was chosen to be 0.011 cm/s. Results from Owen Tube settling experiments were used to assign chem-

ical components of SPM to the slowly- and fast-settling components in the model (Fig. 4.8).

A third component model describes the SPM as a combination of particles that exist either on a seasonal basis or year-round. The benefit of this separation of the SPM is that it enables an explanation of the ranges observed in the short-term variability in different seasons.

4.4 Linking SPM composition to the tides

The limited length of the time series (12 hours; less than one complete tidal cycle) makes it difficult to link SPM variability to tidal cycles in a mathematically rigorous manner. If longer time series were collected, spectral analysis would reveal the primary modes of variation; it is expected that the primary frequencies would be close to the semidiurnal tidal frequencies of ~12.5 h and ~6.25 h. However, because tidal effects at RM53 are so pronounced (Fig. 4.9) it would be highly coincidental if the frequencies of SPM variability and tidal variability were not linked.

Two potential scenarios could account for the observed variability. First, it can be imagined that this variability could be due to an insertion of particles carried with the salt-water into the particle field associated with the river. Depending on the tide, the relative contribution of oceanic particles to the riverine particle field would yield the observed variability. This is a probable process in the Columbia River estuary with a constant daily intrusion of salt water; however, at RM53 there is no salt intrusion, yet tidal and SPM variabilty is still observed. It is thus unlikely that the variability is due to mixing with particles from the ocean end member.

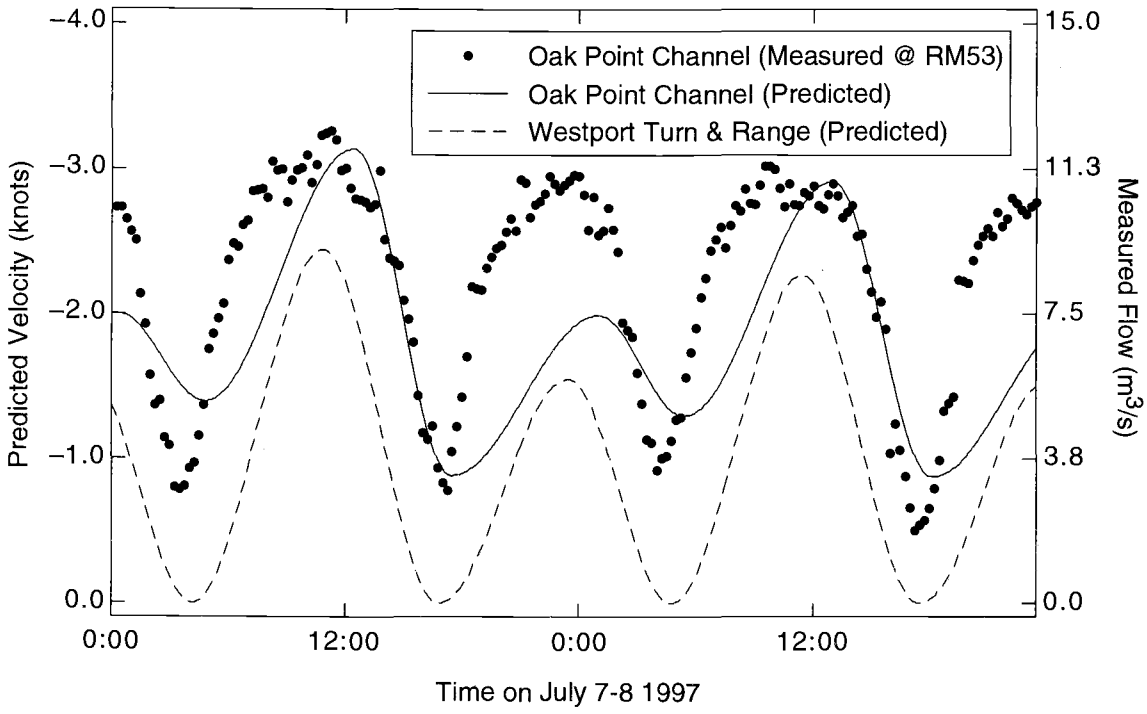

Fig. 4.9: River velocity at RM53 is heavily influenced by tides. Dots show measured flow at RM53 (USGS NASQAN). Predicted river flows (Tides & Currents software package) at Oak Point Channel (RM53 is in this stretch of river) and Westport Turn & Range (immediately downriver of Oak Point Channel) illustrate the time lag between tidally modulated maximum and minimum flows at different locations on the river.

A second possible mechanism, illustrated in figure 4.10, is a tidally driven, differential settling and resuspension model, in which variation in SPM composition and concentration are linked to river velocity. During a flooding tide, the river velocity at RM53 often approaches zero. One can imagine that particle settling and resuspension processes act much differently in this scenario compared to times of high flow (ebbing tide). During low-flow conditions, the larger and denser particles settle, leaving the less dense particles in suspension. Conversely, during high flow, the heavy particles are resuspended and mix with the lighter particles. In reality, the process is probably not so nicely one-dimensional. Resuspension need not be isolated to a resuspension from the bottom. Suspension and

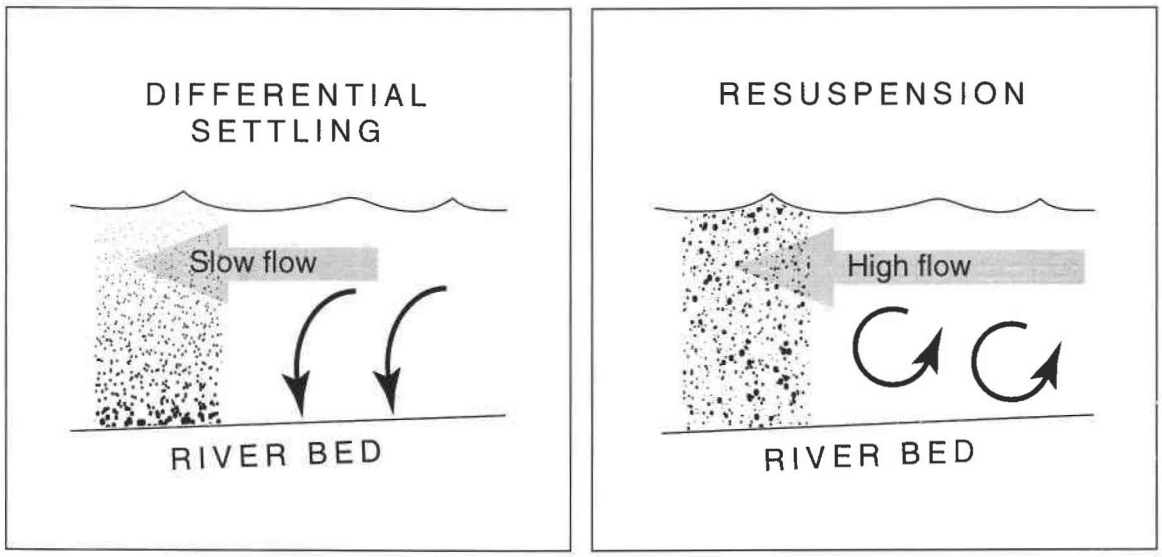

Fig. 4.10: A simplified, 1-D model of settling and resuspension processes that could account for variability of SPM concentration and composition as a result of tidal modulation of river flow.

advection from river banks and floodplains may also contribute to the bulk SPM during high flow periods of the tidal cycle.

The differential settling and resuspension scenario, coupled with the two-component settling model, is consistent with variability in SPM concentration and composition seen at RM53 (Figs. 4.2-4.6). Recall that at mid-depth in the river, bulk SPM concentration was highest during high flow, and lowest during low flow. Conversely, Mn/Al and Chl *a*/ POC were greatest during low flow and least during high flow. Results from the Owen Tube experiments showed that Mn-rich and Chl-rich particles were primarily in the slow settling fractions, while clay minerals and associated POC were in the faster settling fractions. Differential settling of particles during low flow would result in a removal from mid-depth of the heavier particles, which in effect enriches the remaining SPM in manga-

nese and chlorophyll. Then, during high flow, resuspension of the settled particles returns the heavier particles to the mid-depth SPM, decreasing Mn/Al and Chl *a*/POC.

Further evidence in support of the differential settling/resuspension model are the optical backscattering (OBS) versus depth profiles (SPM concentration is approximately 2 x OBS), collected every 30 minutes while at RM53. Two 12-hour time series illustrate the tidal effects on SPM throughout the water column (Fig. 4.11). Though absolute changes in SPM concentration are small (18 - 26 mg/L), the percent changes are significant, and follow a logical progression based on the tides.

At the low-flow period of the tidal cycle (sampling point 99aU1102) the depth profile of SPM shows a lower concentration at the top (20 mg/L) and a higher concentration at the bottom (26 mg/L), consistent with particle settling. Six hours later, at the local maximum in flow (99aU1116), the SPM profile is vertical and nearly constant at 22 mg/L, consistent with resuspension and an even vertical distribution.

4.5 Seasonal effects on settling/resuspension model

The extent to which differential particle settling and resuspension occurs appears to be seasonally dependent. In May 1997 (Fig. 4.2), Chl *a*/POC remained nearly constant over a 12-hour time period, yet two months later (Fig. 4.3) tidal variability in SPM ranged from 20 to 30 mg/g. This same pattern was evident for Mn/Al. By October (Fig. 4.4), variability in Chl *a*/POC and Mn/Al had lessened, and by February 1998 (Fig. 4.5), there was no significant variability.

The seasonal effect on settling/resuspension induced variability is due to seasonal variation in bulk SPM. During early spring, late fall, and winter, little short term variabil-

Fig. 4.11: SPM varies at RM35 in part as a function of tidally modulated river velocity. (a) OBS depth profiles during the 99aU11 time series. (b) OBS depth profiles during the 99aU21 time series.

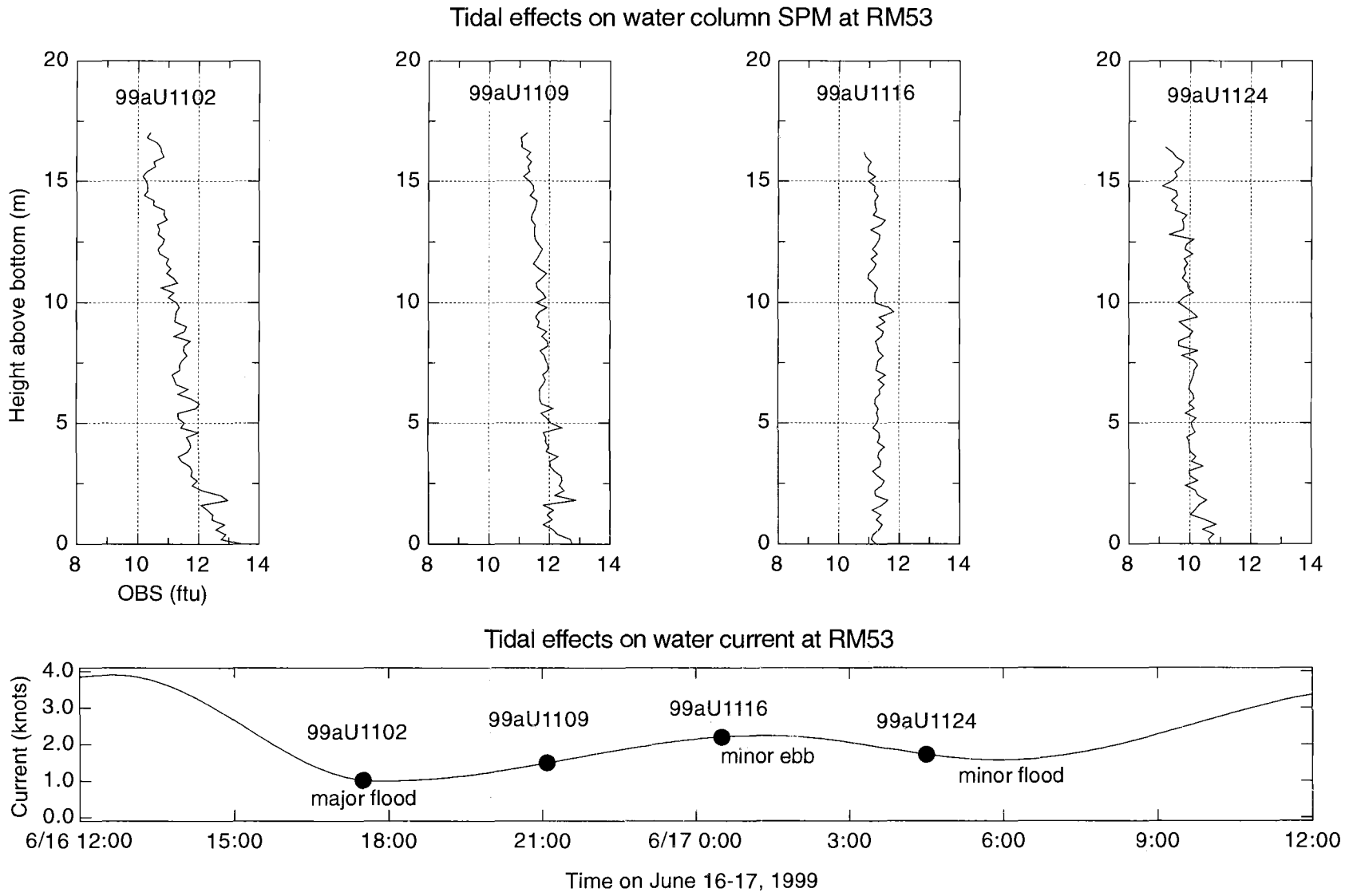
Tidal effects on water column SPM at RM53
99aU1102
99aU1109
99aU1116
99aU1124
Height above bottom (m)
OBS (ftu)
Tidal effects on water current at RM53
Current (knots)
99aU1102
major flood
99aU1109
99aU1116
minor ebb
99aU1124
minor flood
6/16 12:00
15:00
18:00
21:00
6/17 0:00
3:00
6:00
9:00
12:00
Time on June 16-17, 1999

Fig. 4.11

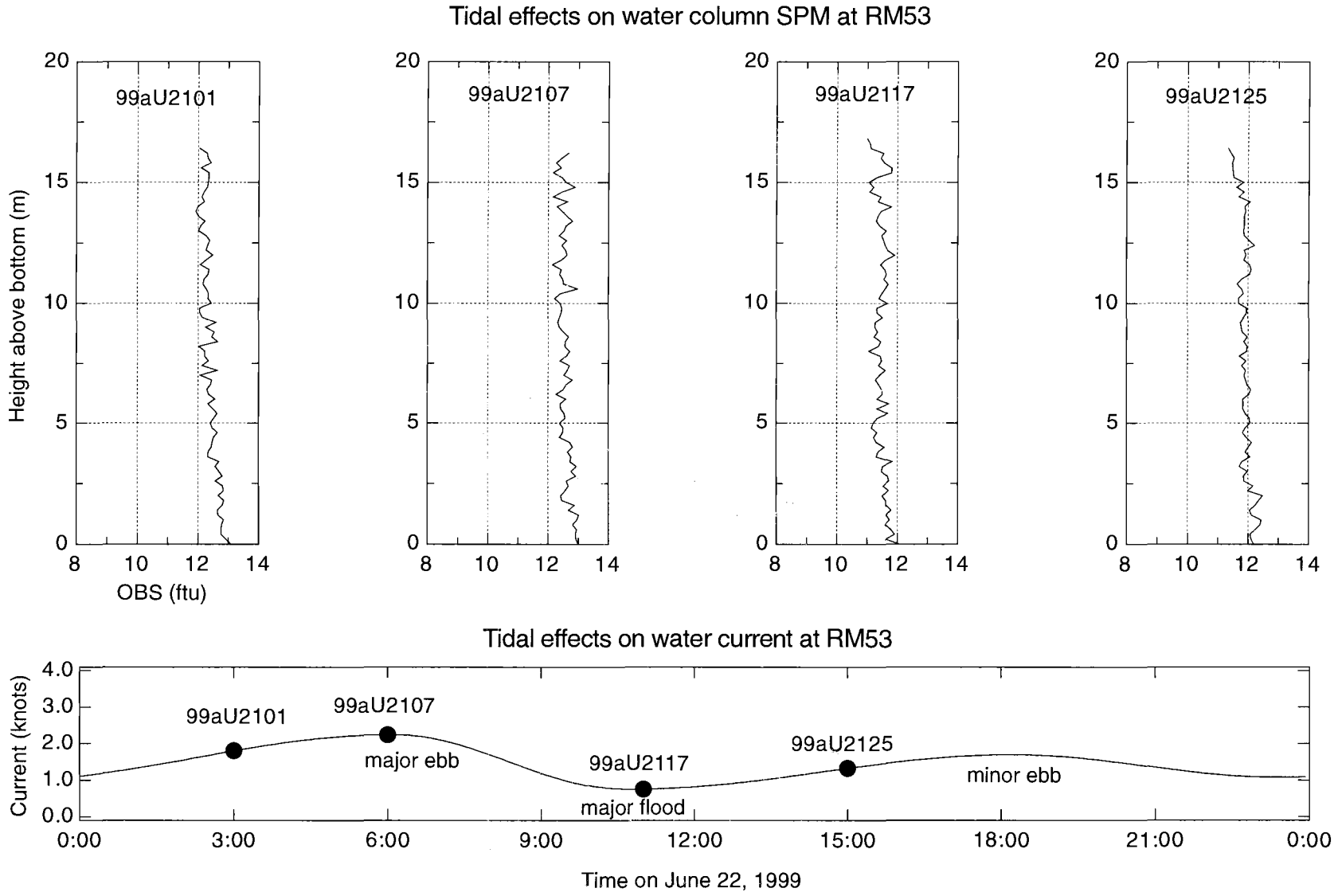

Fig. 4.11 continued

ity in Mn/Al is seen because Mn/Al in bulk SPM is near 0.011; that is, the majority of Mn resides in the heavier aluminosilicate clays. Therefore, a settling of heavy particles cannot result in enrichment of Mn in the slowly-settling material. Likewise, settling of heavy particles cannot yield an enrichment of Chl *a* during the winter in the lighter particles, as most of the POC is detrital in nature and low in Chl *a*.

4.6 Summary

1. Owen Tube settling experiments showed a significant geochemical difference between slowly-settling and fast-settling particles. Slowly-settling particles (<0.11 cm/s) tended to be enriched in Mn and Chl, while fast-settling particles were much more depleted, characteristic of detrital material (aluminosilicate clays and terrestrial POC).

2. SPM composition varied at mid-depth in the Columbia River over 12-hour time periods. This variation is linked to tidally modulated flow in the river. During ebbing tides (high flow) SPM concentrations were greatest, while during low flow they were least. The inverse pattern was seen for both Mn/Al and Chl *a*/POC.

3. A differential particle settling/resuspension mechanism accounts for the short-term variability of SPM concentration and composition at mid-depth in the river. The settling process removes the heavier detrital material, in effect enhancing the concentration of Mn and Chl *a* in the remaining suspension. During resuspension, the heavier particles are reintroduced to the suspension. This process is also significantly effected by seasonal variability in SPM composition.

5: CONCLUSION

5.1 Summary of Observations

1. Seasonal variability of Mn/Al observed by Sullivan in 1995-6 was confirmed in 1999, indicating that the earlier observation was not an artifact of an unusual water year. Data obtained from the USGS for intermediate years improved the confirmation.

2. Electron microprobe was used to generate elemental maps of Columbia River SPM. From these maps, it appears that Mn-rich particles are separate from the aluminosilicate type particles. Results of particles settling experiments with Owen tubes confirms this observation. Reports of mirror image Mn/Al and dissolved Mn variation imply an oxidation and precipitation of dissolved Mn, leading us to believe that the discrete Mn-rich particles seen in Columbia and Willamette river SPM are Mn-oxides.

3. Owen Tube settling experiments showed a significant geochemical difference between slowly-settling and fast-settling particles. Slower settling particles (<0.11 cm/s) tended to be enhanced in Mn and Chl *a*, while faster settling particles were much more characteristic of detrital material (aluminosilicate clays and terrestrial POC).

4. SPM composition varied at mid-depth in the Columbia River over 12-hour time periods. This variation is linked to tidally modulated flow in the river. During ebbing tides (high flow), SPM concentrations were greatest, while during low flow they were least. The inverse pattern was seen for both Mn/Al and Chl *a*/POC.

5. A differential particle settling/resuspension mechanism accounts for the short term variability of SPM concentration and composition at mid-depth in the river. The settling process removes the heavier detrital type material, in effect enhancing the concentration of Mn and Chl *a* in the remaining suspension. During resuspension, the heavier particles are reintroduced to the suspension. This process is also significantly effected by seasonal variability in SPM composition.

5.2 Contaminant transport implications

It was introduced earlier that manganese oxides surfaces are known for their trace metal adsorbing qualities. This fact was one of the drivers of this research. We wanted to determine whether or not the oxides were responsible for seasonal behavior of particulate Mn/Al, and, if in fact oxides were present, how they resided in the SPM. The two main results (1 – that manganese oxides are present in SPM, and 2 – that they exist as small, slowly-settling, discrete particles) are exciting when viewed in the context of contaminant transport into the Columbia River estuary.

Upon entering the estuary, SPM is subjected to a rapidly changing chemical environment, which has the potential to drastically alter the content of SPM. In the case of the Columbia River estuary, the "excess" manganese seen in upriver SPM appears to be lost from the SPM (Fig. 5.1). As SPM is moved through the estuary (increasing salinity) in the south channel, there is a gradual reduction of Mn/Al from values typical of upriver SPM to near crustal abundance. Since the decrease in Mn/Al approaches crustal abundances, it is reasonable to assume that it is the oxide phases of manganese that are being

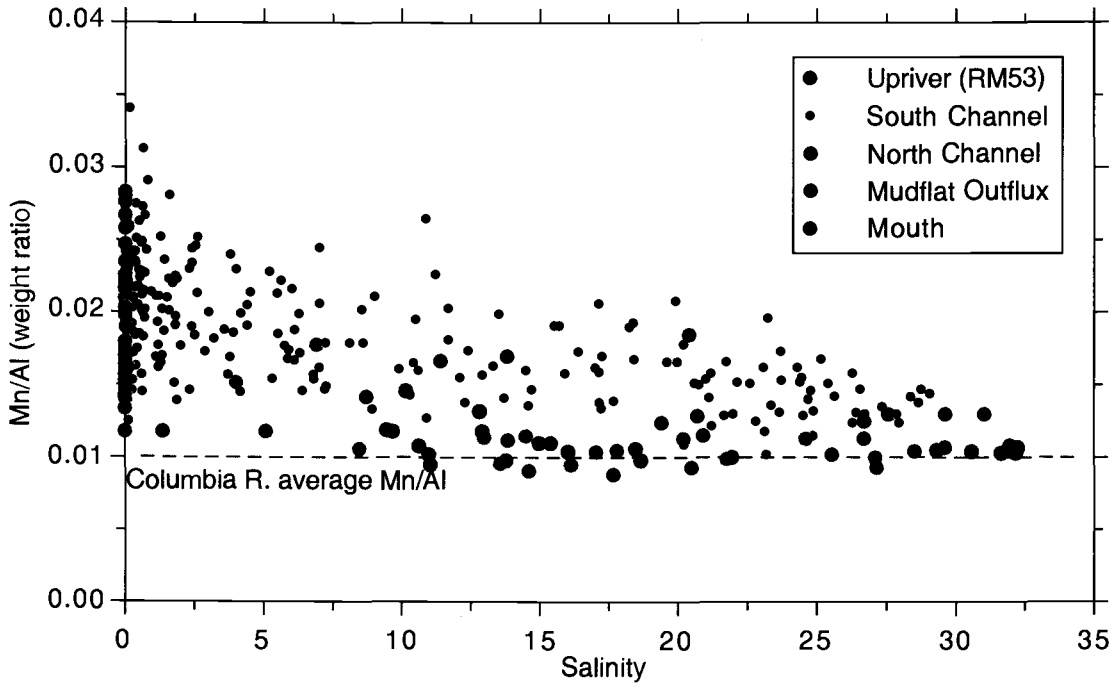

Fig. 5.1: Relationship between salinity and particulate manganese in the Columbia river and estuary (unpublished data, Prahl 1990-1999)

removed from the bulk SPM. The fates of associated trace elements would undoubtedly be tied to this removal.

The following scenario, supported by results of this thesis, could account for the observed oxide removal. Riverborne SPM is introduced to the estuary, flow velocites are slowed considerably, and differential particle settling occurs. During flood tides, a fraction of this freshwater and lighter weight, oxide-rich, suspended material is pushed aside onto intertidal mudflats where its load of SPM partially deposits. Intense bacterial activity and high oxygen demand on the mudflats (Amspoker and McIntire, 1986) leads to reducing conditions (suboxic to anoxic) which facilitates the stripping of manganese oxide from

the particles. Some fraction of the stripped particles subsequently flushed by erosion from the intertidal areas on ebb tides and reintroduced to waters in the central estuary.

The toxicological and environmental aspects of this scenario become evident when one asks the question "What happens to trace metal contaminants adsorbed to the Mn (and Fe) oxide phase of riverborne SPM as this material travels through the freshwater – estuarine gradient?" One possible answer is that the contaminants are released by reductive dissolution of their carrier phase in the intertidal settings. And, in so doing, they are converted to forms with different biological availabilities and possibly with different toxicity characteristics. If intertidal mudflats do act in this way, then we might find ecological consequences in a specific portion of the estuary from pollution problems originating upstream, for instance in Portland.

5.3 Future research

As with all research, a project is never over. There are always unanswered questions, and new paths of inquiry to follow. Listed below are several research directions one might choose to solidify or build upon the results of this thesis.

1. Particle settling experiments and elemental maps of SPM have led us to conclude that "excess" manganese resides in oxide phases. Direct evidence of this, either from selective leaching experiments or powder x-ray diffraction would be quite beneficial.

2. Another unanswered question is what is the mechanism that leads to the seasonal occurence of manganese oxides? Pontér et al. (1992) hypothesize that in the Kalix river

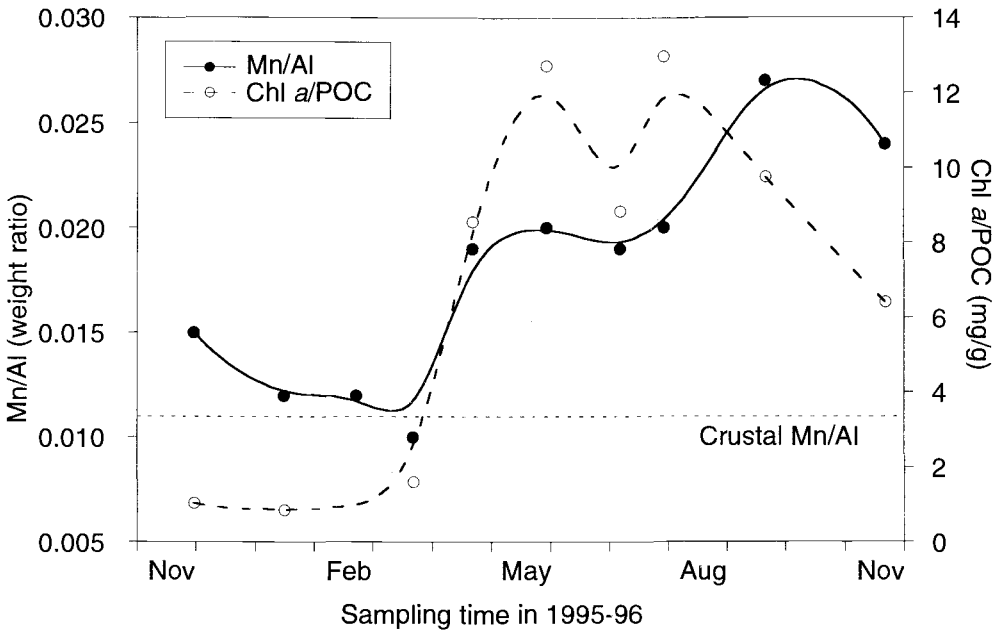

Fig. 5.2: Seasonality in particulate Mn/Al (unpublished data from Sullivan, 1997 study) and Chl *a*/POC (Sullivan et al., 2001) of SPM collected at RM53.

the seasonality in Mn/Al is caused by springtime bacterially mediated oxidation of dissolved manganese, which forms during the winter in numerous lakes along the river system. A similar explanation has been proposed for the St. Lawrence river (Cossa et al., 1990). These conjectures are reasonable given the Mn-oxidizing capabilities of many bacteria (e.g. Cowen and Bruland, 1985) and the energetic benefits of doing so (Sunda and Kieber, 1994), but neither Pontér nor Cossa have evidence to support their hypotheses.

There is limited evidence that a similar bacterial oxidation of dissolved Mn occurs seasonally in the Columbia River, leading to the observed Mn/Al seasonality. The seasonal variability in Mn/Al in the Columbia River correlates with that for Chl *a*/POC (Fig. 5.2). It is known that the rapid increase in Chl *a*/POC is a direct result of spring phytoplankton blooms (Sullivan et al., 2001). It is possible that this correlation is coinciden-

tal. However, it seems more plausible that there is a link between the Mn/Al and Chl *a*/ POC seasonality, and is worth further investigation.

3. A third direction of future research that addresses the issue of contaminant transport is to examine association of anthropogenically introduced trace-elements with different settling fractions of SPM. Do other trace elements preferentially reside in the slowly-settling fractions of SPM, perhaps adsorbed to oxide species? How similar or different are the elemental distributions in riverine and estuarine SPM? Answers to these questions would significantly enhance our understanding of contaminant transport in the Columbia River and potentially other fluvial systems.

REFERENCES

Army Corps of Engineers (1943) A study of methods used in measurement and analysis of sediment loads in streams. pp. 102.

Canfield D. E. (1997) The geochemistry of river particulates from the continental USA: Major elements. *Geochimica et Cosmochimica Acta* **61(16),** 3349-3365.

Cossa D., Tremblay G. H., and Gobeil C. (1990) Seasonality in iron and manganese concentrations of the St. Lawrence river. *The Science of the Total Environment* **97/98,** 185-190.

Cowen J. P. and Bruland K. W. (1985) Metal deposits associated with bacteria: implications for Fe and Mn marine biogeochemistry. *Deep Sea Research.* **32,** 253-272.

Edwards T. K. and Glyson D. G. (1988) Field methods for measurement of fluvial sediment, pp. 118. U.S. Geological Survey.

Ertel J. R. and Hedges J. I. (1985) Sources of sedimentary humic substances: vascular plant debris. *Geochimica et Cosmochimica Acta* **49,** 2097-2107.

Fuhrer G. J., Tanner D. Q., Morace J. L., McKenzie S. W., and Skach K. A. (1996) Water Quality of the Lower Columbia River Basin: Analysis of Current and Historical Water-Quality Data through 1994, pp. 1-157. U.S. Geological Survey.

Gobeil C., Sundby B., and Silverberg N. (1981) Factors influencing particulate matter geochemistry in the St. Lawrence estuary turbidity maximum. *Marine Chemistry* **10(2),** 123-140.

Guézennec L., Lafite R., Dupont J.-P., Meyer R., and Boust D. (1999) Hydrodynamics of suspended particulate matter in the tidal freshwater zone of a macrotidal estuary (the Seine estuary, France). *Estuaries* **22(3A),** 717-727.

Hem J. D. (1978) Redox processes at surfaces of manganese oxide and their effects on aqueous metal ions. *Chemical Geology* **21,** 199-218.

Meybeck M., Cauwet G., Dessery S., Somville M., and Gouleau D. (1988) Nutrients (organic C, P, N, Si) in the eutrophic river Loire (France) and its estuary. *Estuar. Coast. Shelf Sci.* **27,** 595-624.

Niedergesäss R., Eden H., and Schnier C. (1996) Trace element concentrations in suspended particulate matter fractionated according to settling velocity. *Suspended particulate matter in rivers and estuaries,* 41-52.

Niedergesäss R., Racky B., and Schnier C. (1987) Instrumental neutron activation analysis of Elbe River suspended particulate matter separated according to the settling velocities. *Journal of Radioanalytical and Nuclear Chemistry* **114(1),** 57-68.

Odén S. (1924) The size distribution of particles in soils and the experimental methods of obtaining them. *Soil Science* **19(1),** 1-35.

Pontér C., Ingri J., and Boström K. (1992) Geochemistry of manganese in the Kalix river, northern Sweden. *Geochimica et Cosmochimica Acta* **56,** 1485-1494.

Pontér C., Ingri J., Burman J.-O., and Boström K. (1990) Temporal variations in dissolved and suspended iron and manganese in the Kalix river, northern Sweden. *Chemical Geology* **81,** 121-131.

Prahl F. G. and Coble P. G. (1994) Input and behavior of dissolved organic carbon in the Columbia River Estuary. In *Changes in fluxes in estuaries: Implications from science to management* (ECSA22/ERF symposium, Plymouth, September 1992) (ed. K. R. Dyer and R. J. Orth), pp. 451-457. Olsen & Olsen.

Prahl F. G., Small L. F., and Eversmeyer B. (1997) Biogeochemical characterization of suspended particulate matter in the Columbia River estuary. *Marine Ecology Progress Series* **160,** 173-184.

Prahl F. G., Small L. F., Sullivan B. A., Cordell J., Simenstad C. A., Crump B. C., and Baross J. A. (1998) Biogeochemical gradients in the lower Columbia River. Hydrobiologia 261, 37-52.

Reed D. J. and Donovan J. (1994) The character and composition of the Columbia River estuarine turbidity maximum. In *Changes in fluxes in estuaries: Implications from science to management* (ECSA22/ERF symposium, Plymouth, September 1992) (ed. K. R. Dyer and R. J. Orth), pp. 445-450. Olsen & Olsen.

Reed S. J. B. (1993) Electron Microprobe Analysis. Cambridge University Press, Cambridge University, 326 pp.

Rickert D. A., Petersen R. R., McKenzie S. W., Hines W. G., and Wille S. A. (1977) Algal Conditions and the Potential for Future Algal Problems in the Willamette River, Oregon, pp. 1-39. U.S. Geological Survey.

Shiller A. M. (1997) Dissolved trace elements in the Mississippi River: Seasonal, interannual, and decadal variability. *Geochimica et Cosmochimica Acta* **61(20),** 4321-4330.

Simenstad C. A., Reed D. J., Jay D. A., Baross J. A., Prahl F. G., and Small L. F. (1994) Land-Margin Ecosystem Research in the Columbia River Estuary: an interdisciplinary approach to investigating couplings between hydrological, geochemical and ecological processes within estuarine turbidity maxima. In *Changes in fluxes in estuaries: Implica-*

tions from science to management (ECSA22/ERF symposium, Plymouth, September 1992) (ed. K. R. Dyer and R. J. Orth), pp. 437-444. Olsen & Olsen.

Stumm, W., J. J. Morgan. (1970). Aquatic Chemistry. Wiley, New York, N.Y., 583 pp.

Sullivan B. E. (1997) Annual Cycles of Organic Matter and Phytoplankton Attributes in the Columbia and Willamette Rivers, with Reference to the Columbia River Estuary. Masters, Oregon State University.

Sullivan B. E., Prahl F. G., Small L. F., and Covert P. A. (2001) Seasonal Variations in Suspended Particle and Freshwater Phytoplankton Input to the Columbia River Estuary. *Geochimica et Cosmochimica Acta* **65(7),** 1125-1139.

Sunda W. G. and Kieber D. J. (1994) Oxidation of humic substances by manganese oxides yields low-molecular-weight organic substrates. *Nature* **367,** 62-64.

Sundby B. and Silverberg N. (1981) Pathways of manganese in an open estuarine system. *Geochimica et Cosmochimica Acta* **45,** 293-307.

Turner A. (1996) Trace-metal partitioning in estuaries: importance of salinity and particle concentration. *Marine Chemistry* **54,** 27-39.

Whetten J. T., Kelley J. C., and Hanson L. G. (1969) Characteristics of Columbia River Sediment and Sediment Transport. *Journal of Sedimentary Petrology* **39(3),** 1149-1166.

Williams M. R. and Millward G. E. (1998) Dynamics of Particulate Trace Metals in the Tidal Reaches of Ouse and Trend, UK. *Mar. Poll. Bull.* **37(3-7),** 306-315.

APPENDICES

Table A.1: Suspended particulate matter in the Columbia and Willamette Rivers

Date	Temp. (°C)	pH	SPM (mg/L)	POC (mg/L)	PON (mg/L)	Chl *a* (µg/L)	Al (wt%)	Cu (ppm)	Fe (wt%)	Mn (ppm)	Zn (ppm)
Columbia River @ RM53 (Beaver Army Terminal)											
29-Mar-99	7.3	8.12	16.9	0.61	0.059	4.38	8.8	100	5.05	1269	316
20-Apr-99	9.9	8.12	15.6	0.64	0.076	12.64	8.4	413	4.46	1348	490
11-May-99	11.0	8.12	12.1	0.82	0.099	18.05	7.0	116	4.41	1478	327
25-May-99	13.9	7.94	14.3	0.45	0.054	6.76	8.0	171	4.03	1220	247
08-Jun-99	13.9	7.78	20.4	0.89	0.100	13.25	7.4	93	4.17	1428	259
22-Jun-99	16.1	7.83	20.9	0.83	0.105	17.04	8.9	–	4.97	1641	–
03-Aug-99	20.3	7.83	12.0	0.86	0.096	11.15	7.6	–	4.62	1637	–
14-Sep-99	18.9	7.85	10.4	0.63	0.076	13.62	7.7	–	4.48	1653	–
12-Oct-99	14.4	7.85	–	0.39	0.053	7.01	–	–	–	–	–
30-Nov-99	9.8	7.33	47.7	1.07	0.103	2.83	9.4	–	5.89	1092	–
Willamette River @ WRM12.8 (Morrison Bridge, Portland, OR)											
30-Mar-99	8.2	7.49	12.2	0.60	0.059	3.31	10.4	–	7.34	1298	–
19-Apr-99	12.3	7.49	7.3	0.42	0.046	6.31	10.3	–	7.06	2979	–
24-May-99	13.4	7.30	9.0	0.62	0.056	4.32	8.4	–	5.65	2070	–
21-Jun-99	15.2	7.31	6.2	0.47	0.057	5.76	8.7	–	5.72	2790	–
02-Aug-99	21.7	7.31	8.4	0.66	0.099	9.67	8.7	–	5.96	3701	–
13-Sep-99	18.4	7.32	7.3	0.47	0.058	2.72	8.8	–	5.69	3942	
18-Oct-99	13.6	7.69	–	0.34	0.037	3.00	–	–	–	–	–
15-Nov-99	12.0	7.17	17.9	0.54	0.060	3.38	11.6	–	7.81	1707	–
13-Dec-99	8.1	7.06	–	–	–	1.14	–	–	–	–	–

Table A.2: Twelve hour time series at RM53.

Sample Code	Time	SPM (mg/L)	POC (mg/L)	PON (mg/L)	Chl *a* (µg/L)	Al (wt%)	Cu (ppm)	Fe (wt%)	Mn (ppm)	Zn (ppm)
May 3-4, 1997										
97aU1101M	11:18 PM	25.8	1.042	0.118	6.65	7.90	–	5.53	1412	269
97aU1105M	1:07 AM	31.6	1.198	0.132	7.16	6.38	–	5.18	1278	259
97aU1109M	3:07 AM	39.1	1.207	0.144	7.16	7.04	–	5.05	1270	233
97aU1113M	5:02 AM	26.3	1.193	0.145	7.70	6.89	–	5.01	1236	201
97aU1117M	7:06 AM	26.7	1.417	0.151	8.47	7.78	–	5.30	1305	210
97aU1121M	9:03 AM	30.0	1.229	0.146	8.12	8.63	–	5.60	1467	207
May 15, 1997										
97aU2101M	5:07 AM	28.4	1.137	0.144	10.88	–	–	–	–	–
97aU2105M	7:06 AM	34.8	1.339	0.160	11.36	–	–	–	–	–
97aU2109M	9:05 AM	31.0	1.221	0.150	10.95	–	–	–	–	–
97aU2113M	11:04 AM	29.8	1.284	0.138	11.76	–	–	–	–	–
97aU2117M	1:04 PM	41.3	1.355	0.146	11.88	–	–	–	–	–
97aU2121M	3:05 PM	30.1	1.199	0.138	11.39	–	–	–	–	–

Table A.2, Continued

Sample Code	Time	SPM (mg/L)	POC (mg/L)	PON (mg/L)	Chl *a* (µg/L)	Al (wt%)	Cu (ppm)	Fe (wt%)	Mn (ppm)	Zn (ppm)
July 7-8, 1997										
97bU1101M	5:09 PM	18.1	1.230	0.191	23.91	7.22	–	4.61	1576	275
97bU1105M	7:04 PM	27.1	1.082	0.155	26.62	7.56	–	4.73	1498	244
97bU1109M	9:03 PM	22.9	1.290	0.158	27.52	6.69	–	4.42	1485	217
97bU1113M	11:04 PM	30.0	1.094	0.167	23.91	5.64	–	4.07	1219	197
97bU1117M	1:05 AM	23.2	0.928	0.144	25.01	6.97	–	4.74	1641	227
97bU1121M	3:04 AM	23.0	0.988	0.165	26.43	4.77	–	4.02	1318	211
97bU1125M	5:06 AM	22.4	1.116	0.177	25.26	8.03	–	4.94	1634	248
October 6, 1997										
97cU1101M	11:08 AM	36.0	1.098	0.098	6.86	6.61	–	3.46	1071	127
97cU1105M	1:06 PM	28.7	0.867	0.083	8.12	7.14	–	3.87	1157	148
97cU1109M	3:05 PM	25.2	0.736	0.074	7.67	8.44	–	4.35	1471	171
97cU1113M	5:05 PM	17.2	0.541	0.071	6.54	8.35	–	3.45	989	127
97cU1117M	7:04 PM	18.8	0.640	0.092	6.68	8.29	–	4.00	1298	154
97cU1121M	9:06 PM	23.3	0.664	0.092	7.22	6.55	–	3.11	878	110
97cU1125M	11:03 PM	26.4	0.755	0.111	7.76	7.35	–	3.83	1213	141

Table A.2, Continued

Sample Code	Time	SPM (mg/L)	POC (mg/L)	PON (mg/L)	Chl *a* (µg/L)	Al (wt%)	Cu (ppm)	Fe (wt%)	Mn (ppm)	Zn (ppm)
February 21-22, 1998										
98aU1101M	12:10 PM	10.9	0.784	0.112	6.70	8.71	2467	5.95	1316	–
98aU1105M	2:05 PM	10.2	0.708	0.084	7.05	8.59	1968	5.93	1328	–
98aU1109M	4:05 PM	11.9	0.639	0.056	6.55	8.52	1707	5.84	1302	–
98aU1113M	6:04 PM	15.3	0.724	0.112	5.84	8.88	2114	5.68	1316	–
98aU1117M	8:05 PM	14.4	0.707	0.070	6.34	8.40	1649	5.39	1185	–
98aU1121M	10:05 PM	15.1	0.568	0.102	6.20	8.32	1545	5.30	1187	–
98aU1125M	12:05 AM	14.1	0.624	0.075	5.70	8.48	1335	5.55	1199	–
June 22, 1999										
99aU2101M	3:00 AM	16.9	0.835	0.099	20.20	6.44	–	4.24	1496	214
99aU2105B	5:00 AM	16.5	0.811	0.099	18.50	6.77	–	4.44	1553	–
99aU2105M	5:00 AM	21.8	0.887	0.104	19.30	6.61	–	4.16	1350	194
99aU2105T	5:00 AM	23.7	0.725	0.091	21.00	6.93	–	4.24	1321	–
99aU2109M	7:00 AM	22.8	0.760	0.095	19.50	6.48	–	4.10	1296	184
99aU2113M	9:00 AM	16.6	0.719	0.088	22.30	8.19	–	5.22	1886	250
99aU2115M	10:10 AM	16.1	0.809	0.096	–	7.08	–	4.55	1623	203
99aU2117M	11:00 AM	17.1	0.750	0.094	23.60	7.17	–	4.48	1620	215
99aU2121M	1:00 PM	17.8	0.781	0.092	20.10	7.79	–	4.73	1636	230
99aU2125M	3:00 PM	15.5	0.777	0.093	19.20	6.96	–	4.36	1613	223

Table A.3: Owen Tube fraction data from RM53

Station	Fraction	Fraction Volume (mL)	SPM (mg/L)	POC (mg/L)	PON (mg/L)	Chl *a* (µg/L)	ΣCH_2O (mg/L)	Al (wt%)	Mn (wt%)	Fe (wt%)
95U1125B	1&2	512	31.0	1.06	0.15	25.4	–	6.47	0.125	–
	3&4	512	35.0	0.94	0.13	25.6	–	6.46	0.123	–
	5&6	512	16.0	0.88	0.13	25.2	–	7.00	0.154	–
	7&8	611	10.0	0.63	0.11	23.4	–	6.70	0.164	–
96U1105M	1	256*	37.3	2.69	0.27	18.0	–	8.31	0.131	–
	2	256*	49.3	1.80	0.20	20.4	–	7.68	0.142	–
	3	256*	27.3	1.30	0.14	17.9	–	7.75	0.151	–
	4	256*	14.7	0.95	0.11	14.9	–	7.62	0.163	–
	5&6	512*	11.3	0.85	0.10	15.2	–	6.85	0.155	–
	7&8	611*	13.7	0.84	0.09	14.7	–	6.12	0.138	–
96U1121M	1	256*	86.5	4.52	0.46	19.8	–	7.37	0.124	–
	2	256*	75.0	2.72	0.29	19.4	–	7.84	0.132	–
	3	256*	45.0	1.43	0.17	16.9	–	7.11	0.121	–
	4	256*	19.7	1.04	0.13	14.1	–	6.29	0.141	–
	5&6	512*	13.8	0.93	0.12	13.4	–	7.60	0.155	–
	7&8	611*	12.6	0.84	0.11	16.0	–	7.52	0.159	–

* Actual bottle volumes were not recorded. Values used in Odén calculations are based on measured volumes of 95U1125B.

Table A.3, continued

Station	Fraction	Fraction Volume (mL)	SPM (mg/L)	POC (mg/L)	PON (mg/L)	Chl *a* (µg/L)	ΣCH_2O (mg/L)	Al (wt%)	Mn (wt%)	Fe (wt%)
99aU1109M	1&2	490	66.0	1.57	0.17	26.8	0.90	7.94	0.134	4.87
	3&4	495	22.7	0.77	0.09	22.9	0.54	7.17	0.150	4.71
	5&6	505	10.0	0.57	0.07	16.6	0.37	7.34	0.206	5.21
	7&8	585	3.4	0.36	0.06	18.6	0.32	8.05	0.355	8.50
99aU1121M	1&2	490	44.7	1.56	0.18	19.3	1.13	6.92	0.156	4.83
	3&4	505	12.0	0.63	0.08	16.9	0.31	6.51	0.196	5.05
	5&6	515	11.3	0.62	0.07	14.8	0.25	3.35	0.132	3.50
	7&8	580	6.9	0.45	0.06	13.5	0.31	3.79	0.168	4.15
99aU2105M	1&2	870	113.3	2.61	0.25	24.6	0.93	8.91	0.111	4.46
	3&4	1015	34.7	0.99	0.11	18.7	0.45	7.11	0.112	4.01
	5&6	995	13.3	0.73	0.08	19.1	0.35	7.65	0.161	4.35
	7&8	1180	6.7	0.60	0.07	15.3	0.32	10.5	0.247	6.35
99aU2115M	1&2	865	92.7	2.23	0.23	22.1	1.15	7.69	0.125	4.65
	3&4	1050	17.3	0.89	0.10	20.2	0.57	5.42	0.136	4.29
	5&6	950	9.3	0.73	0.07	17.5	0.43	4.97	0.161	5.13
	7&8	1160	8.7	0.68	0.06	16.3	0.37	1.88	0.110	2.98

Table A.4: Geochemistry of SPM fractionated according to settling velocity.

Station	Settling Fraction (cm/s)	SPM (mg/L)	POC (mg/L)	PON (mg/L)	Chl *a* (µg/L)	ΣCH_2O (mg/L)	Al (wt %)	Mn (wt %)	Fe (wt %)
95U1125B	∞ -> .22	0.13	0.04	0.005	0.09	–	9.77	0.391	–
	.22 -> .044	5.95	0.03	0.001	0.00	–	5.95	0.088	–
	.044 -> .011	6.32	0.06	0.002	0.55	–	6.95	0.125	–
	.011 -> 0	10.00	0.74	0.120	24.20	–	6.70	0.164	–
96U1121M	∞ -> .22	6.90	0.43	0.040	0.53	–	6.55	0.136	–
	.22 -> .044	11.80	0.19	0.019	1.32	–	7.84	0.107	–
	.044 -> .011	0.74	0.05	0.006	0.23	–	5.56	0.159	–
	.011 -> 0	12.70	0.86	0.112	13.10	–	7.65	0.159	–
99aU1109M	∞ -> .22	9.72	0.19	0.017	–	0.074	8.54	0.131	4.98
	.22 -> .044	6.46	0.11	0.010	–	0.093	6.42	0.091	4.23
	.044 -> .011	2.50	0.06	0.003	–	0.019	11.00	0.187	4.84
	.011 -> 0	5.71	0.44	0.064	–	0.336	6.34	0.249	6.04

Table A.4, continued

Station	Settling Fraction (cm/s)	SPM (mg/L)	POC (mg/L)	PON (mg/L)	Chl *a* (µg/L)	ΣCH_2O (mg/L)	Al (wt %)	Mn (wt %)	Fe (wt %)
99aU1121M	∞ -> .22	7.78	0.22	0.024	0.47	–	6.74	0.134	4.54
	.22 -> .044	0.47	0.01	0.005	1.08	–	42.15	0.951	24.52
	.044 -> .011	0.95	0.03	0.004	0.42	–	8.05	0.138	4.04
	.011 -> 0	8.89	0.53	0.067	14.00	–	3.19	0.144	3.64
99aU2105M	∞ -> .22	15.40	0.33	0.028	1.28	0.097	9.74	0.110	4.65
	.22 -> .044	10.70	0.13	0.015	0.18	0.049	7.66	0.091	4.15
	.044 -> .011	2.80	0.06	0.004	0.21	0.022	3.17	0.055	1.78
	.011 -> 0	9.18	0.64	0.076	17.50	0.323	8.95	0.198	5.31
99aU2115M	∞ -> .22	15.40	0.28	0.026	0.37	0.119	8.51	0.125	4.89
	.22 -> .044	4.67	0.09	0.013	0.95	0.061	4.67	0.098	2.91
	.044 -> .011	0.37	0.03	0.008	1.21	0.049	55.07	0.764	32.60
	.011 -> 0	8.72	0.69	0.064	16.30	0.375	2.33	0.123	3.43

APPENDIX B: ELECTRON MICROPROBE IMAGES

97aU2105M.E

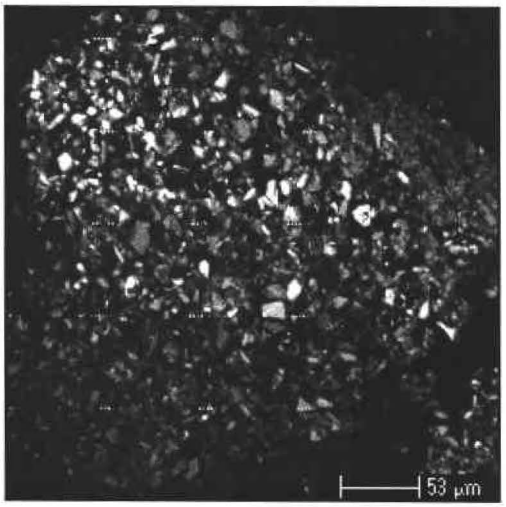

Aluminum

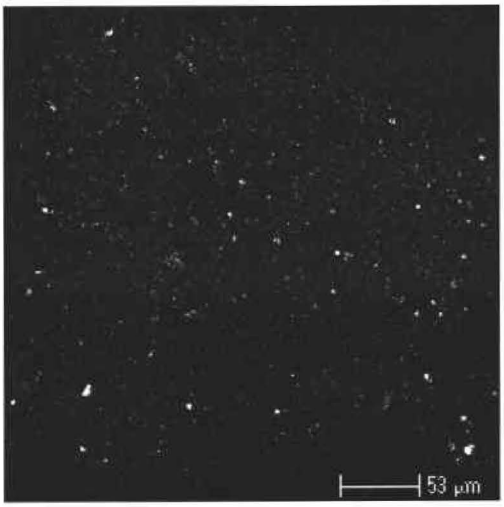

Manganese

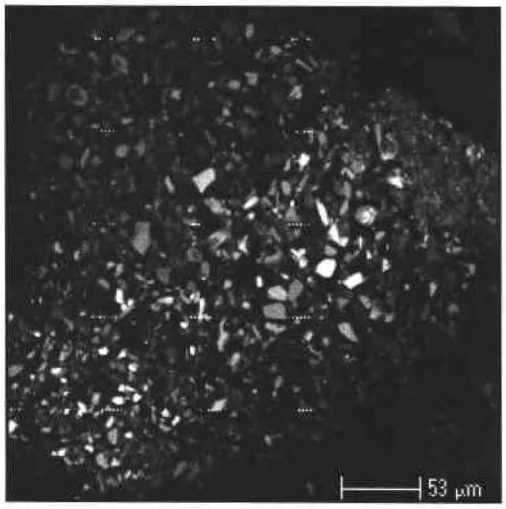

Silicon

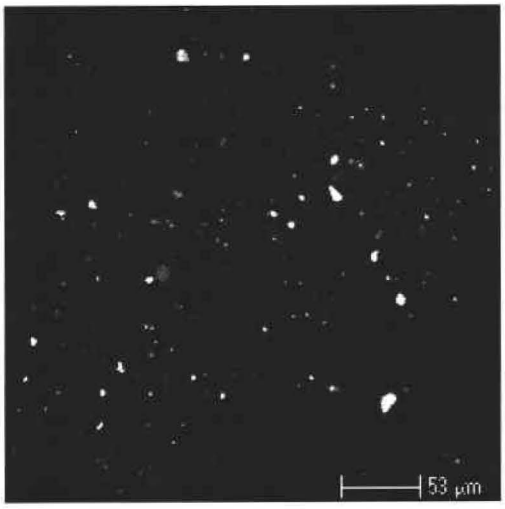

Titanium

97aU2105M.E1

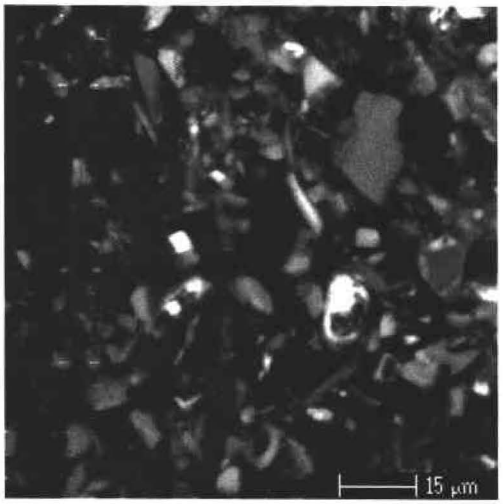

Aluminum

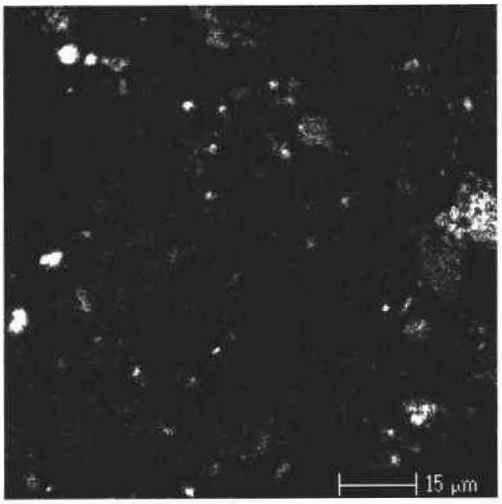

Manganese

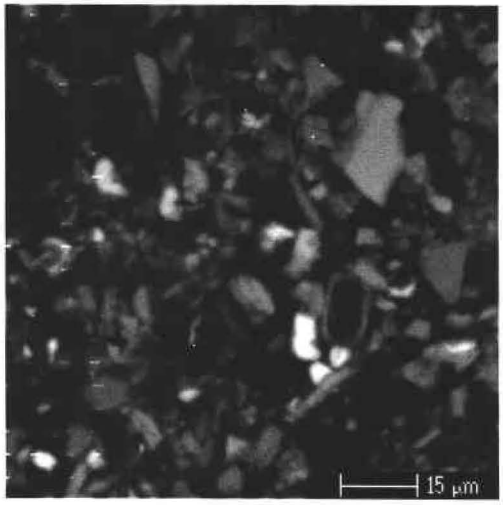

Silicon

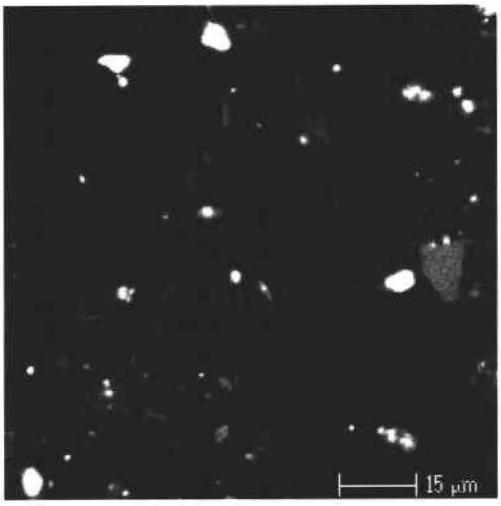

Titanium

97bU1125M.C

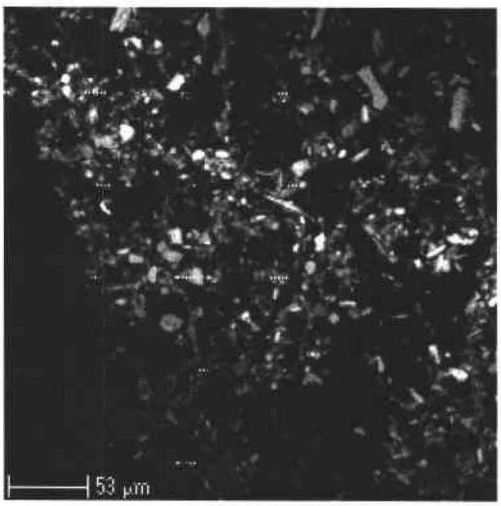

Aluminum

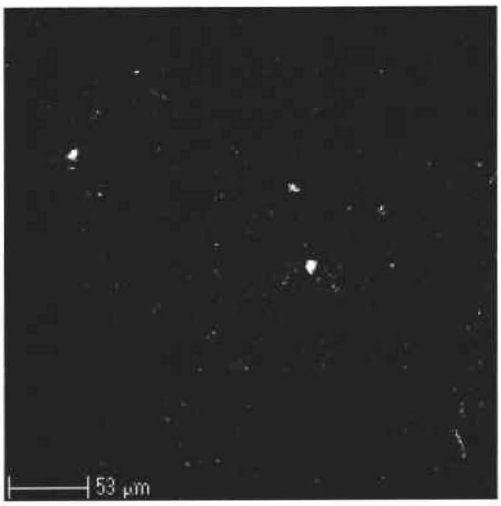

Manganese

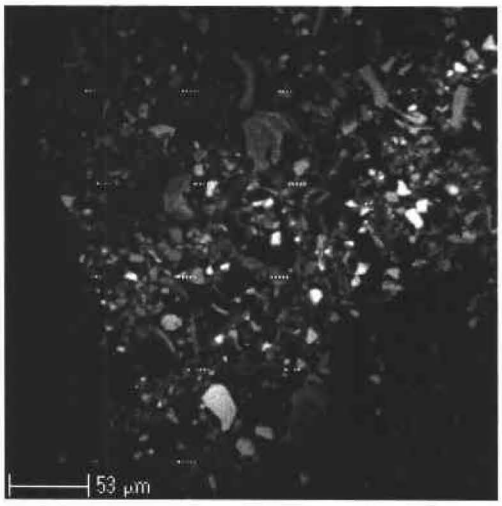

Silicon

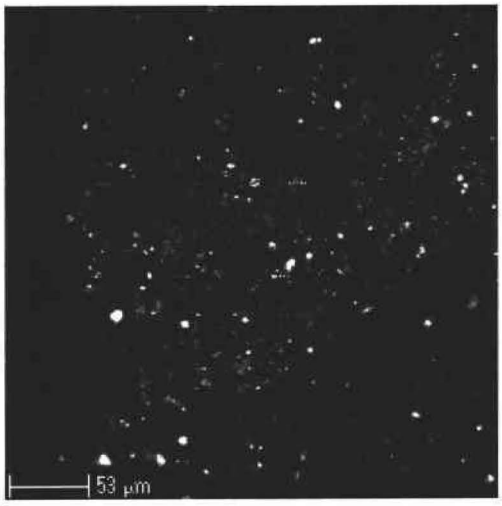

Titanium

97bU1125M.D

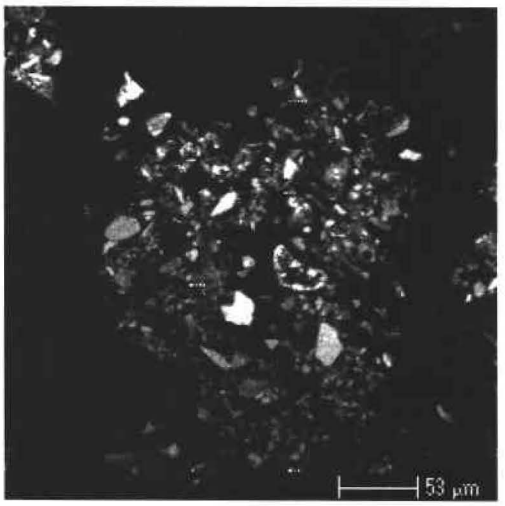

Aluminum

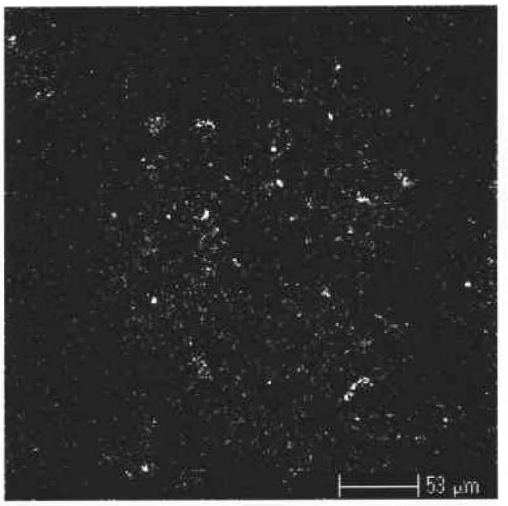

Manganese

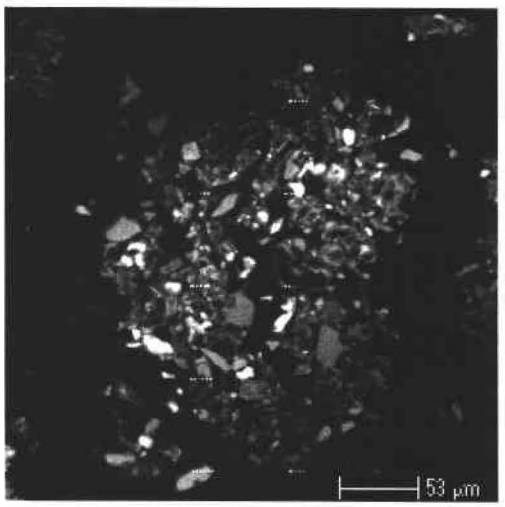

Silicon

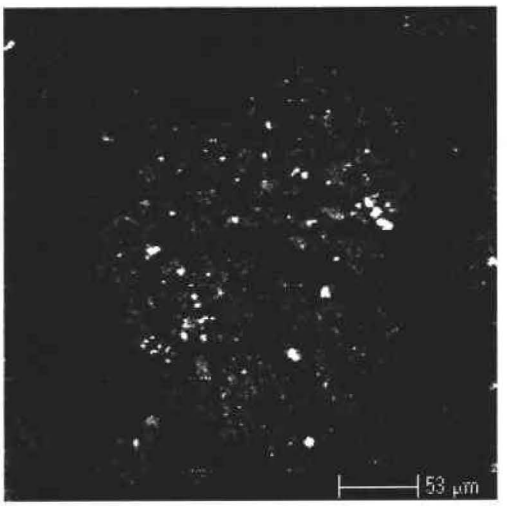

Titanium

97bU21125M.E

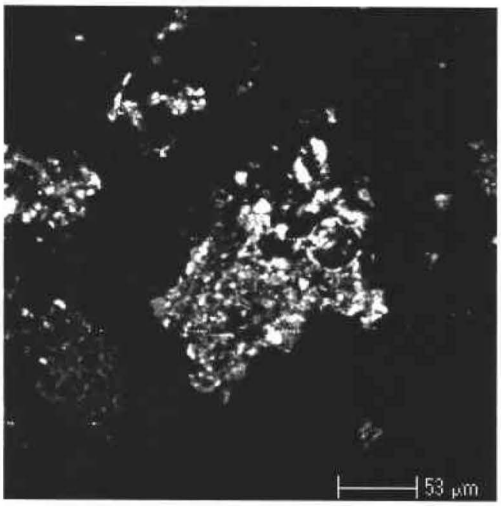

Aluminum

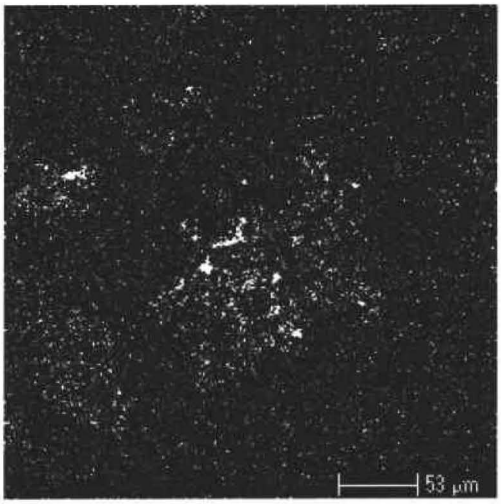

Manganese

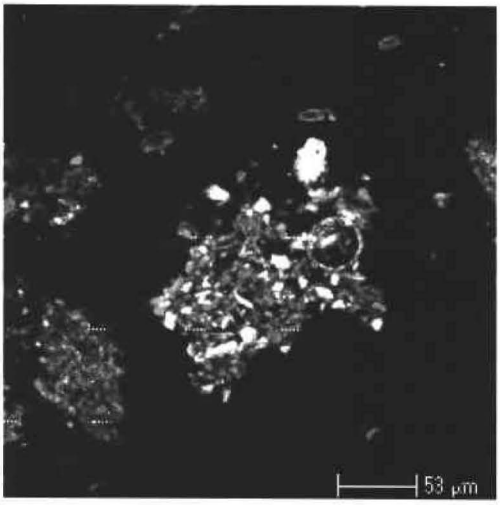

Silicon

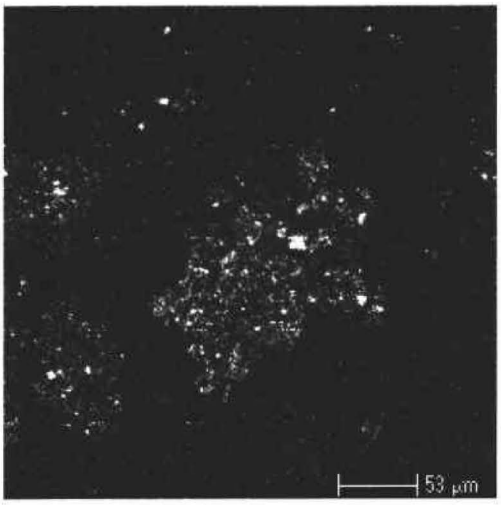

Titanium

97cU1109M.A

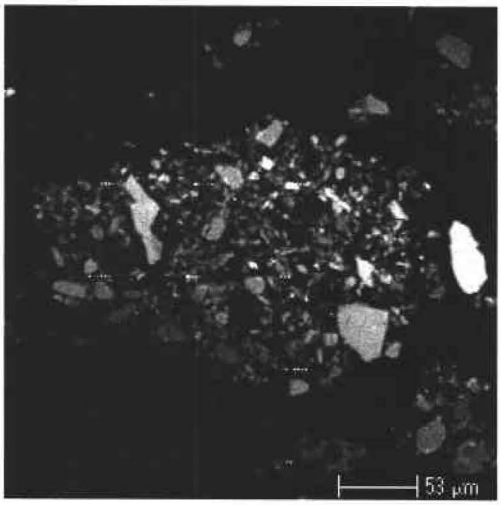

Aluminum

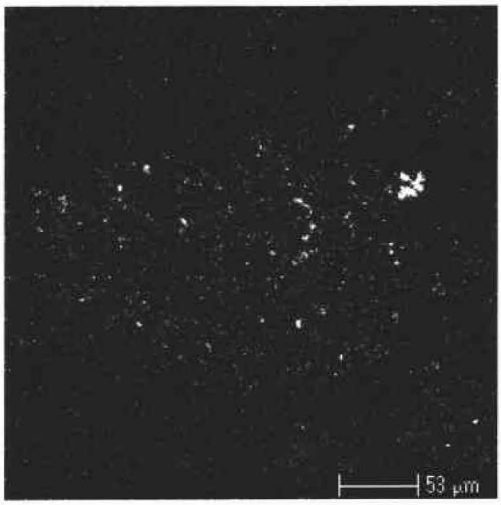

Manganese

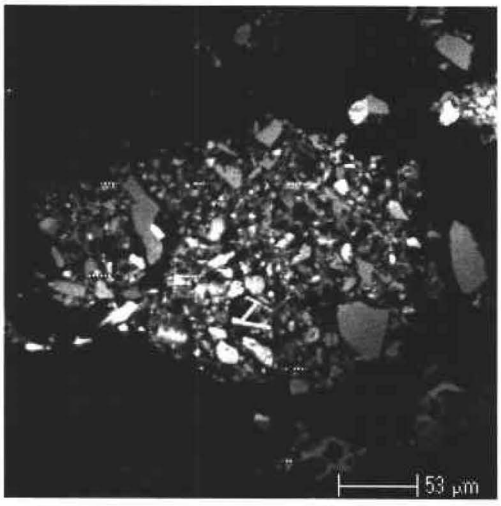

Silicon

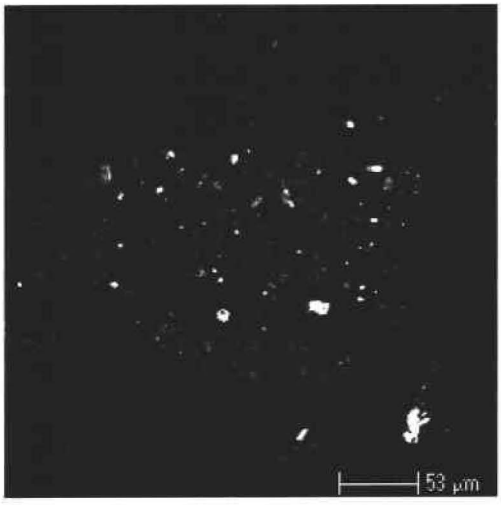

Titanium

97cU21109M.D

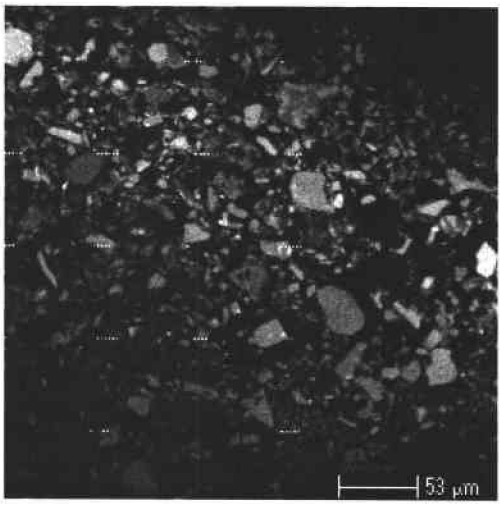

Aluminum

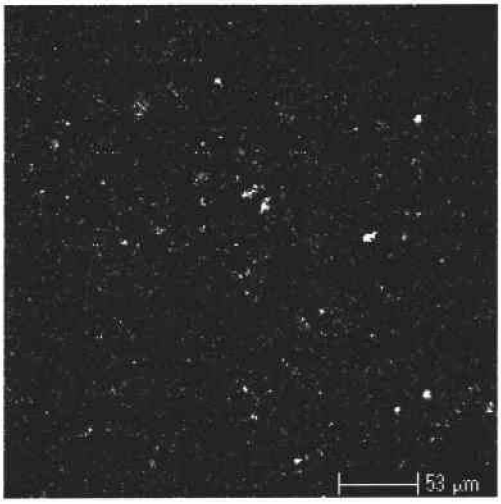

Manganese

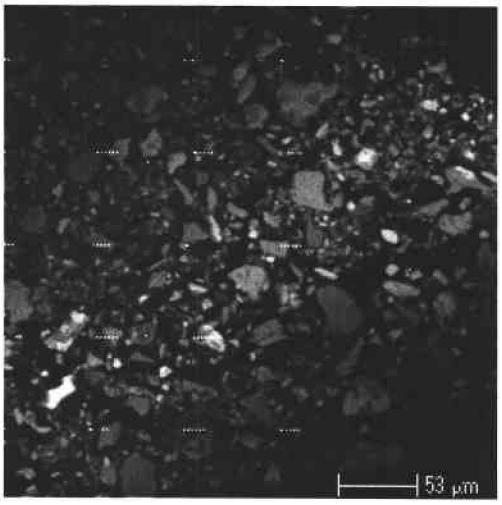

Silicon

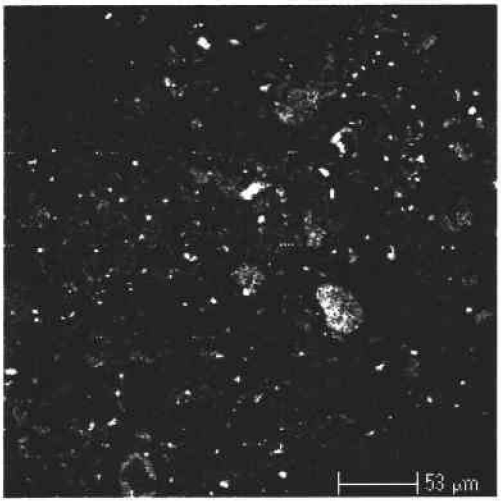

Titanium

97cU1109M.E

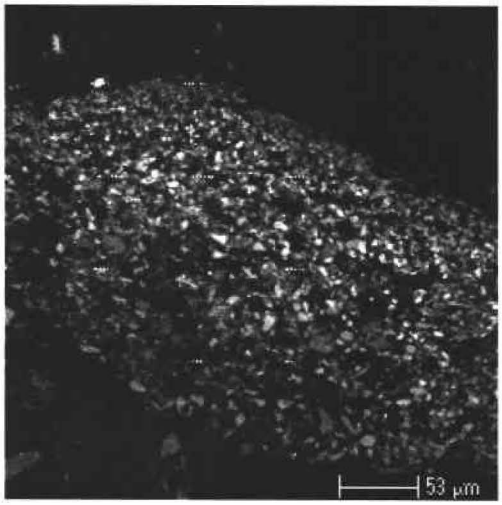

Aluminum

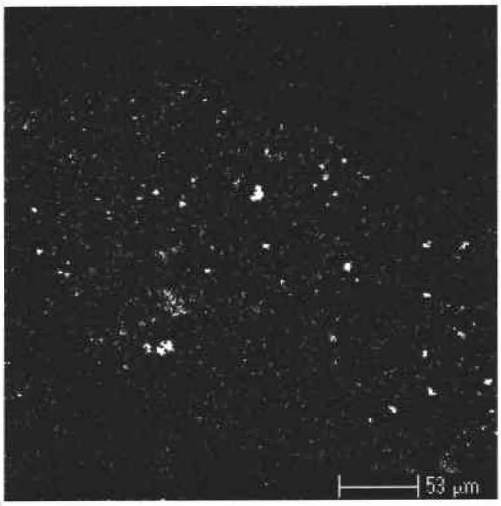

Manganese

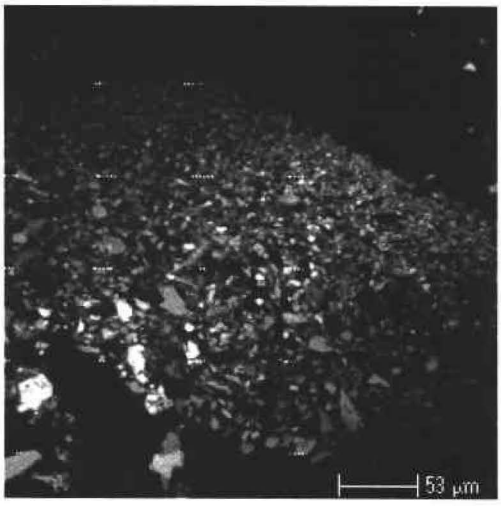

Silicon

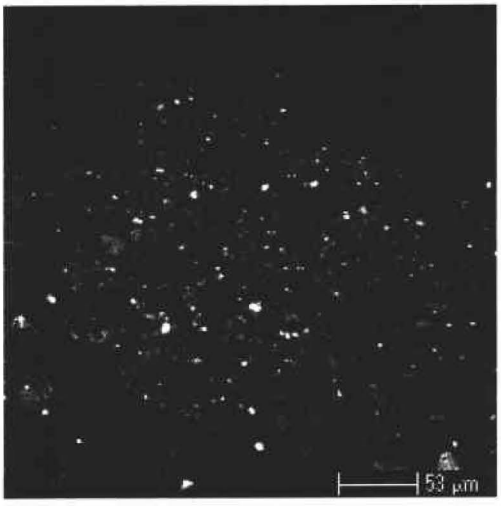

Titanium